1-1-2013

Effects of DNA Damage and CDK Inhibitors on the Nucleoli

Vineet Garg
University of South Carolina

EFFECTS OF DNA DAMAGE AND CDK INHIBITORS ON THE NUCLEOLI

By

Vineet Garg

Bachelor of Technology

Guru Gobind Singh Indraprastha University, 2009

Master of Technology

Guru Gobind Singh Indraprastha University, 2011

Submitted in Partial Fulfillment of the Requirements

For the Degree of Master of Science in

Pharmaceutical Sciences

College of Pharmacy

University of South Carolina

2013

Accepted by:

Igor Roninson, Major Professor

Lorne Hofseth, Committee Member

Douglas Pittman, Committee Member

Lacy Ford, Vice Provost and Dean of Graduate Studies

DEDICATION

To my beloved Family

for their everlasting love and support

ACKNOWLEDGEMENT

I am very thankful to my major professor Dr. Igor Roninson for giving me an opportunity to work under his guidance. His way of accomplishing the work and immense determination will amaze and inspire me for the rest of my life.

I am sincerely thankful to Dr. Eugenia Broude for her incessant efforts to develope me as the part of the esteemed lab group.I want to specially thank Dr. Gary P. Schools for his esteemed mentorship. I consider myself very lucky to have worked with him. I will always remember him as my friend and mentor.

I wish to extend my sincere thanks to all research scholars and lab mates,, Dr. Chang-uk Lim, Dr. Mengqian (Max) Chen, Dr. Zhengguan Yang, Frederico Parez, Tiffanie Aiken, Jenny Hentz, Dr. Martina McDermott, Jiaxin Liang (Jason), Dr. Donald Porter, Dr. Serena Altilia, Vimala Kaza, Pratik Patel, Alex Chumanevich, Dr. Michael Shtutman, Dr. Elina Levina, Dr. Hao Ji (Emily) for their help and guidance. I thank my friends and colleagues Arpit, Kamaljeet, Saptaparnee, Tracy, Katie, David and Anusha for their support and motivation. I thank Mrs. Diane Wise and Mrs. Carolyn risinger for their constant help.

I am indebted to my family for their love and care. I thank everyone who has been linked to this project in some way and those who helped me in presenting this manuscript in its present form and most of all the Almighty for his blessings.

ABSTRACT

The nucleolus is the primary site of ribogenesis and consists of three compartments, namely, fibrillar center (FC), dense fibrillar component (DFC) and granular component (GC). Recent studies have observed a novel structure distinct from these three compartments which forms in the nucleolus upon DNA damage called Intranucleolar body (INoB). Previous studies in our laboratory have found INoBs forming in HT1080 fibrosarcoma cell lines after ectopic overexpression of damage-inducible cell cycle inhibitor p21. This INoB formation has been observed to be decreased by Senexin A which is an inhibitor of transcription regulating kinases CDK8/CDK19.

Here we show that INoB formation correlates with the level of p21 induction in HT1080 fibrosarcoma cells. Similarly, induction of other CDK inhibitors such as p16 and p27 also causes INoB formation which was significantly decreased by Senexin A treatment in case the cells where p16 is overexpressed. DNA damage by doxorubicin also caused the formation of INoBs in HCT116 colon carcinoma cells which was decreased by Senexin A treatment. CDK8 was found to be localized in these INoBs. Comparative studies in HCT116 wt and HCT116 p21-/- cells showed a partial requirement of p21 for DNA damage induced INoB formation and also indicated a possibility of different type

of INoBs which we called ‘type 2 INoBs’ which did not contain CDK8 and could arise in the absence of p21

INoB formation was not observed in quiescent cells. Protein content of CDK8, RNA polymerase I and, to a lesser extent, RNA polymerase II was found to be higher in nucleolar extracts of HT1080 cells with p21 overexpression. This indicates that rRNA transcription may be linked to INoB formation and associated changes in the nucleolus. p21 overexpression also caused RNA polymerase I localization at the foci on the periphery of the nucleolus, separate from INoBs, which we called ‘Pol I aggregates’. Formation of these Pol I aggregates in p21 overexpressed cells was decreased by CDK8 inhibition with Senexin A. INoB formation was not found to be correlated with senescence-associated β-Gal staining (SA-β-Gal), one of the markers of the senescent phenotype, and SA-β-Gal expression was unaffected by Senexin A. However, Senexin A treatment significantly reduced the increase in the cell size in p21-overexpressing HT1080 cells, a characteristic feature of senescence, which is indicative of continued protein synthesis and ribogenesis in senescent cells.

This study reveals additional information regarding the nucleolar restructuring after DNA damage or p21 expression, which may be related to rRNA transcription and cell senescence.

TABLE OF CONTENTS

LIST OF FIGURES

CHAPTER 1

INTRODUCTION

1.1 Nucleolus

1.1.1 Historical perspective

The nucleolus was first observed as an ovoid body in the nucleus in the eighteenth century. Felice Fontana noted its occurrence in the slime of an eel and reported it in his paper on the venom of vipers. The nucleolus remained unstudied for almost a century but with the progress of light microscopy many cytologists observed its dynamic nature during cell division. In 1934, nucleolar organizing region (NOR) was found to be involved in the formation of nucleolus during telophase. Within four decades, RNA was detected in the nucleolus and ribosomal genes (rDNA) were identified in the NOR with the help of *in situ* hybridization techniques [1, 2]. Nucleolar segregation and extraction was made possible in the following years. After that, many studies focusing on characterization of proteins present in the nucleolus were done and soon it was proposed that the nucleolus may be the site of ribogenesis. With the introduction of better techniques in electron microscopy, study of the functional organization of many proteins in the nucleolus became feasible. In recent years, several proteins which are not related to ribogenesis have been identified [3] in the nucleolus which suggest its function in other biological processes.

1.1.2 Function of the Nucleolus

The nucleolus is the primary site of ribogenesis and, in fact, it is formed by the act of producing ribosome [4]. It is not bound by a membrane and therefore does not have the hydrophobic barrier a lipid membrane provides. Its active period can be observed by its size. In mammalian cells, it disappears at the beginning of the cell cycle and gets reorganized during the telophase of mitosis. However, in yeast it is active during all cell cycle stages.

Transcription of rDNA takes place in the nucleolus giving rise to the 47S precursor ribosomal RNAs (pre-rRNAs). Then, these pre-rRNAs are processed and finally assembled with 80 ribosomal proteins and 5S RNA to form two subunits of the eukaryotic ribosome (40S and 60S). As evident from the yeast studies, this whole process is under the control of 150 small nucleolar RNAs (snoRNAs) and two ribonucleoprotein complexes. Consistent with the two subunits, there is a small subunit processosome (SSU) with U3 snoRNAs and 40 proteins for 40S subunit and a large subunit processosome (LSU) for 60S ribosomal subunit [5].

1.1.3 Structure of Nucleolus

Electron micrograph of the nucleolus shows the presence of three different compartments within the nucleolus: the Fibrillar centers (FCs), the Dense fibrillar component (DFC) and the Granular component (GC). The FCs can be seen as clear areas within the nucleolus surrounded by the DFC. The FC and the DFC are present in the GC (Figure 1.1(a)). A condensed chromatin network can be seen at the boundary of the nucleoplasm and the nucleolus and this can be seen

using standard staining methods. When assessed by light microscopy, DNA staining by DAPI usually excludes nucleolus as the amount of DNA inside the nucleolus is low.

This compartmentalization is related to the function of the nucleolus as the ribosome synthesis factory. The FC and the DFC boundary is the site of rDNA transcription and hence give rise to the 47S pre-rRNA [6]. RNA polymerase I is the marker of FC and transcribes gene coding for rRNA (Figure 1.1(b)). The DFC is the site of pre-RNA processing. The processing of this pre-rRNA takes place during its migration from DFC to GC. rRNA processing proteins nucleolin and fibrillarin localize in the DFC region. Fibrillarin (rRNA 2'-O-methyltransferase fibrillarin) is involved in the first step of RNA processing and is associated with U3 snoRNAs and is a marker for the DFC region (Figure 1.1(b)). The GC does not possess any nascent RNA transcripts [7]. Although processing of most of the rRNA starts in the DFC, GC is the region where final assembly of the rRNA with the ribonucleoproteins takes place. Nucleolar phosphoprotein B23 or nucleophosmin is the marker of GC region [8] (Figure 1.1(b)). These markers provide an effective way to distinguish the different compartments of the nucleolus and also to monitor any defect in the ribogenesis process.

1.2 Nucleolar changes under stress

The nucleolus is a dynamic organelle that based on recent studies seems to be involved in many functions other than ribogenesis. A proteomic analysis of over 4500 nucleolus-associated proteins hints towards additional roles of nucleolus required for the functioning of the cell [9]. Although 30% of the proteins

have functions related to the different steps of ribosome subunit synthesis, other proteins have been linked with processes like biosynthesis of multiple RNPs, regulation of cell cycle, apoptosis, response to viral infection and DNA repair [10].

The relation of the nucleolus and cellular stress is also evident from the changes in the content of different nucleolar proteins under stress conditions. Proteomics studies have been performed to analyze the dynamics of the nucleolar proteome in response to the DNA damage. These studies used mass spectrometry based SILAC (stable isotope labeling by amino acids in cell culture) quantitative proteomics method for characterizing the nucleolar proteome and its dynamics under DNA damaging conditions [11]. This study demonstrated the spatial reorganization of the proteins in the nucleolus as compared to cytoplasm and nucleus following etoposide-induced DNA damage which poisons topoisomerase II hence introducing double stranded breaks [12].

Fluorescent microscopy techniques have been used to measure the levels and locations of more than 1000 endogenously tagged proteins in individual living cells before and after topoisomerase I poison camptothecin (CPT) treatment [13]. This method showed the changes in the protein localization under DNA damage. Interestingly, many of the proteins observed to undergo changes under the stress conditions are of nucleolar origin.

Various types of changes in morphology of the nucleolus are also observed when a cell is under stress. The first type is nucleolar segregation which is caused by DNA damage through UV irradiation or topoisomerase II poison such as etoposide and/or transcriptional inhibition (e.g., by actinomycin D)

[14]. Nucleolar segregation is characterized by the condensation and separation of the FC and GC (Figure 1.2 (middle panel)) [15]. The formation of ‘‘nucleolar caps’’ around the nucleolus is also observed although not identifiable in this particular figure (Figure 1.2). The second type of change in nucleolar morphology is nucleolar disruption leading to unraveling of FC which occurs when RNA polymerase II or protein kinases are inhibited (Figure 1.2 (right panel)) [16]. DRB (5,6-dichloro-1-b-D-ribobenzimidazole) is a kinase inhibitor which inhibits RNA polymerase II transcription and leads to nucleolar disruption.

Nucleolus morphology has also been studied in other types of stress. Apart from inhibition of RNA polymerase II and protein kinases nucleolar disruption is observed following treatment with DNA damaging agents such as ionizing radiation (IR), camptothecin and bleomycin or stress such as heat shock, hypoxia and treatment with 5-fluorouracil [17-23]. 5-fluorouracil causes the inhibition of DNA and RNA synthesis. Changes in nucleolar morphology are also observed during many viral infections such as adenovirus, polio virus and HIV [24].

1.3 The Intranucleolar Body (INoB)

Intranucleolar bodies are novel observations of abnormal structures in the nucleolus. These are almost spherical structures, which look like indentations (0.5-4µm) in the differential interference contrast (DIC) images, but are really inclusions within the nucleolus (Figure 1.3)

Nucleolar aggresomes are formed by an inhibited proteasome [25]. Many proteins such as p21, several cyclins and CDKs get aggregated in these

aggresomes where they cannot be actively degraded by the proteasome machinery [26]. It is currently unclear how the composition of nucleolar aggresomes differs from INoBs.

Intranucleolar bodies were also observed by another group studying the localization of p21 in relation with nucleolar export to the cytoplasm. They treated cells with doxorubicin, also known as Adriamycin, which is a topoisomerase II cleavable complex stabilizing agent which causes double-stranded breaks in the DNA. They observed that when HCT116 cells were treated with 258 nM doxorubicin for 48 hours p21 was localized in the nucleus in 80% of the cells [27]. Among this 80% of cells, 50% had p21 in the nucleolus in the form of round (spherical) aggregates surrounded by a halo of free fluorescent signal which they named INoBs (Figure 1.4(a)). Accumulation of p21 in INoBs after DNA damage was also observed in other cell lines in addition to HCT116 colorectal cell line. MCF7, WI38 and 1306 cells also showed an increased expression of endogenous p21 after doxorubicin treatment and p21 accumulation in INoBs. Although they reported the localization of p21 in the INoBs they did not address what was causing the formation of these INoBs. The question if DNA damage was the reason of this INoBs formation was not asked. They also observed these structures as circular structures inside the nucleolus in the phase contrast images (Figure 1.4(a,b,c)). This localization was not only observed in the case of doxorubicin treatment but also when other DNA damage agents, such as ultraviolet (UV) light exposure and cisplatin were used (Figure 1.4(b,c)). UV irradiation causes the formation of covalent adducts between adjacent

pyrimidines on the DNA strands which eventually result in double-stranded and single- stranded breaks in DNA, while cisplatin causes the formation of DNA adducts by cross-linking adjacent guanines.

Electron micrographs also show the formation of these INoBs in HCT116 cells treated with doxorubicin for 24 hours (Figure 1.5(a)). INoBs are different from all previously characterized compartments of the nucleolus such as fibrillar center (FC), dense fibrillar component (DFC) and granular component (GC) (Figure 1.5(b)). Immunogold labeling of p21 confirms that it localizes in the INoB upon doxorubicin treatment (Figure 1.5(c)). .

Another group has observed structures similar to INoBs which they also called intranucleolar bodies with a different acronym, INBs. They observed these structures in a region distinct from FC, DFC and GC. They performed immunocytochemistry localization studies and found many proteins localizing in these structures which are involved in DNA repair and replication, protein turnover, RNA processing and chromatin organization [28]. They used the localization of PA28γ which is the nuclear isoform of the 11S proteasome activator complex as the criterion for identifying and characterizing the INBs (Figure 1.6(a)).

They also analyzed the effect of different DNA damaging agents on the frequency of INBs. HeLa cells were exposed to an ionizing radiation (IR) dose of 10 Gy, left to recover for 3 h, and subsequently analyzed by indirect immunofluorescence. They showed an increase from 40% to 75% in the number of cells having INB (Figure 1.6(b)). Also, HeLa cells were treated with 50 μM

etoposide (eto) for 3 hours or with either 25 nM camptothecin (CPT) or 2 mM hydroxyurea (HU) for 24 hours, and analyzed by indirect immunofluorescence. All the treatments caused a significant increase in the number of cells with PA28γ positive INBs (Figure 1.6(b)). Etoposide is an inhibitor of topoisomerase II similar to doxorubicin used in our experiments but only a 3 hour treatment was performed as compared to much longer treatment time from 24 to 48 hours in our experiments. Camptothecin is a topoisomerase I inhibitor and hydroxyurea stalls the replication fork during the DNA replication process. All these reagents cause the formation of double stranded breaks in the DNA.

We have reasons to believe that the INBs may be different from INoBs. Firstly, they did not show any characterization of INBs in the phase contrast images or differential interference contrast (DIC) images which was used by Abella et. al [27] and our laboratory as the primary criteria for the recognition of INoBs. Secondly, there are a high percentage of cells (30-40%) with INBs in the untreated control condition which is very high as compared to only up to 10% INoB positive cells in control seen in our results. Thirdly, they didn't show any localization of p21 or CDK8 in these INBs which is observed in the INoBs following DNA damage in the Abella et. al paper [29] and our laboratory's results. Lastly, they see a very low frequency of cells (<20%) with INBs and a decrease in the frequency of cells with INB upon UV treatment or 1 µM NQO treatment for 3 hours (Figure 1.6(b)). Although Abella et. al did not compare the number of cells with INoBs in UV treated versus untreated cells, they observed that p21

localized in INoBs in almost 50% of the HCT116 cells which exogenously expressed HA-p21 [27].

Studies performed in our laboratory with a HT1080 cell line which expresses p21 in response to IPTG (Isopropyl β-D-1-thiogalactopyranoside) showed that INoBs arise after p21 is induced by treatment with 50μM IPTG for 48 hours. Also p21 and CDK8 were shown to be co-localized in these INoBs (Figure 1.7(a)). Time lapse microscopy demonstrated that after the addition of 50 μM IPTG the initiation of INoBs formation happens at approximately 24 hours post treatment (Figure 1.7(b)). When IPTG treated cells were scored for the presence of INoBs and the localization of p21 and CDK8 in the nucleoli, we observed that both INoB formation and localization of p21 and CDK8 was reduced significantly by 10 μM CDK8 inhibitor Senexin A treatment (Figure 1.7(c)). This observation indicates that p21 and CDK8 may be required for the formation and yet unidentified function(s) of these INoBs.

1.4 Cyclin Dependent Kinases inhibitors (CKIs)

Cyclin dependent kinases (CDK) involved in the regulation of cell cycle are CDK1, CDK2, CDK4 and CDK6 [30]. These kinases associate with proteins called cyclins which act as activators and hence CDK can cause the respective kinase activity. Cyclin dependent Kinase inhibitors (CKIs) can cause growth arrest by interacting with these CDK/cyclin complexes. Quiescence cells' reversible growth arrest can be resumed by providing the required growth conditions. When quiescent cells are stimulated to proliferate, CDK4 and CDK6 are activated by interacting with a D-type cyclin. The activity of these protein

complexes (CDK4–6/Cyclin D kinases) is followed by the subsequent activation of the CDK2 which associate with cyclin A and E, which in turn stimulate the initiation of DNA replication. Upon completion of DNA replication, CDK1/cyclin B kinases are activated which is followed by the M-phase or the mitotic phase.

1.4.1 CKIs and cell growth arrest pathways

CDK inhibitors regulate the activity of the CDK and cyclin complexes and cause the cell cycle arrest at particular points in response to various signals or the absence of appropriate conditions required for the normal cell proliferation. In mammalian cells, CDK inhibitors can be divided into two families: cip/kip family and INK4 family. The cip/kip family consists of p21, $p27^{Kip1}$ and $p57^{Kip2}$ while the INK4 family has four related proteins namely $p16^{INK4a}$ (also known as MTS1, CDK4I and CDKN2), $p15^{INK4b}$ (also known as MTS2), $p18^{INK4c}$, and $p19^{INK4d}$ [31]. p16 was the first characterized member of the INK4 family and was isolated based upon its interaction with and inhibition of CDK4 [32]. The blockage of CDK-mediated phosphorylation which inhibits the tumor suppressor protein retinoblastoma (Rb) is the primary mechanism for growth arrest induced by CDK inhibitors. Rb is converted to its active hypophosphorylated form, which sequesters and hence inhibits E2F transcription factors that are necessary for DNA replication and cell cycle progression [33]. The INK4 family of CKIs inhibits the CDK4–6 kinases through the retinoblastoma pathway (Figure 1.8(a)). p16 is a CKI which acts as a tumor suppressor and is found to be non-functional in around 30% of human tumors [34]. p16 levels are upregulated during senescence which is required for the maintenance of growth arrest in those cells

[35, 36]. Also, studies show that the oncogene Bmi-1 can downregulate the expression of p16 [37].

p27 has been shown to be related to senescence in murine and human fibroblasts. Phosphatase and tensin homolog (PTEN) is a phosphatase which dephosphorylates 3,4,5-trisphosphate (PIP3) into Phosphatidylinositol 4,5-bisphosphate (PIP2), thus counteracting the activity of the Phosphatidylinositide 3-kinases (PI3K) [38]. The oncogenic nature of PI3K has been ascribed to regulatory subunit p85 [39]. Overexpression of PTEN or inhibition of PI3K can lead to the upregulation of p27 in response to decreased levels of PIP3 [40]. Another study shows that the lifespan of the human fibroblasts is reduced by an early onset of senescence after PI3K inhibition [41]. All these observations fits into the hypothesis that high levels of p27 contribute to senescence through the pathway described (Figure 1.8(b)).

p53 is a tumor suppressor inactivated in many kinds of cancers. p53 is a negative regulator of the cell cycle, which is induced by different factors with DNA damage being the most studied stimulus. Activation of p53 is responsible for the induction of growth arrest in senescent cells. During replicative senescence, p53 levels are regulated through ubiquitination and subsequent protein degradation. MDM2 protein is the ubiquitin E3 ligase which controls the degradation of p53. On the other hand, p14ARF, a tumor suppressor sequesters the Mdm2 protein hence increasing the p53 levels (Figure 1.8(c)) [42]. Also, promyelocytic leukemia (PML) tumor suppressor stimulates p53 during replicative and RAS-induced accelerated senescence through p53 acetylation [43, 44]. The activated

p53 has multiple effects on gene expression including transcriptional activation of p21 (Figure 1.8(c)) [45]. However, p21 can be induced by p53 dependent and independent processes [46].

Overexpression of p21 in the dividing cells by ectopic methods can lead to growth arrest in G1 and G2 phase [47] [48]. Other than the retinoblastoma pathway, p21 can affect transcription of genes by other processes. The effect of p21 has been explained through the interaction of CDK2 with transcriptional co-factor p300 that augments NFkB (nuclear factor kappa-light-chain-enhancer of activated B cells) and other inducible transcription factors [49]. p21 also interacts with c-Jun amino-terminal kinases, apoptosis signal-regulating kinase 1 and Gadd45. The C-terminal portion of p21, which binds the proliferating cell nuclear antigen (PCNA) and is not involved in CDK inhibition, is required for the inhibition of keratinocyte differentiation markers by p21 [50].

1.4.2 *p21 overexpression from an inducible promoter in HT1080 p21-9 cells*

Gene expression can be artificially turned on and off using promoters that incorporate the bacterial LacI repressor by using a physiologically neutral agent IPTG in the HT1080 human fibrosarcoma cell line used in most of our experiments [51]. HT1080 p21-9 cell line was derived previously in our laboratory from HT1080 3'SS6 cells after transduction with retroviral vector LNXCO3 carrying the coding sequence of the human p21 gene under the IPTG-inducible promoter [52]. HT1080 3'SS6 cells carry the LacI repressor hence we can use IPTG, which is a neutral β-galactoside, for regulated expression of promoters coupled with lac operator sequences. Also, p16 and p27 were expressed in

HT1080 cells from a similar IPTG inducible retroviral vector LNXRO2 [52]. p21 induction can be performed in HT1080 p21-9 cells by the treatment with 50 µM IPTG (Figure 1.9(a)), and this induction is accompanied by rapid (within 14 h) termination of DNA replication (Figure 1.9(b)) and mitosis (Figure 1.9) [53]. Analysis of thymidine [^{3}H] incorporation by autoradiography for radioactive analogue of hydrogen, tritium [^{3}H] into the DNA during DNA replication determines the level of DNA synthesis in the cells.

1.4.3 CKIs and Cell Senescence

Untransformed mammalian primary cells in culture can only undergo a finite number of cell divisions known as the Hayflick limit [54]. After the Hayflick limit the cells become growth arrested permanently. This permanent growth arrest is known as replicative senescence. This gradual process in human cells has been attributed to the shortening and other structural changes of telomeres which are present at the chromosomal ends [55]. This process involving changes in the structure of telomeres resemble DNA damage or in some cases are actually caused by DNA damage [56, 57]. DNA damage was also found to induce rapid cell growth arrest in cultured cells. This growth arrest was different from replicative senescence and had different phenotypic characteristics [55, 58]. This new type of senescence which can be called “accelerated senescence” does not involve telomere shortening and can also be initiated in normal proliferating cells by the expression of mutant Ras or Raf [59, 60]. The “accelerated senescence” is referred to as senescence/cellular senescence in the rest of this text unless specified otherwise. The study of cellular senescence in cultured cells and its

related features is an important experimental system for understanding cancer development.

Senescence in general is an irreversible type of growth arrest which can happen due to many reasons and through many pathways. The different pathways involved in growth arrest by CKIs such as p21, p27 and p16 are summarized in Figure 1.10. Under the effect of DNA damage or population doublings (Hayflick limit) a cell can undergo either accelerated or replicative senescence involving p21 activation through p53. Gradually the p21 levels go down and p16 levels rise to maintain the growth arrest during senescence (Figure 1.10).

The inhibition of senescence in the cells by mutations in key regulatory components of these pathways can lead to their division beyond normal limits and consequently give rise to tumors. On the other hand, senescent cells remain metabolically and synthetically active and show a characteristic senescent phenotype which includes increase in cell size, flattening and granularity [61]. The senescent cells can be identified by using SA-β-Gal staining which reacts with X-Gal (5-bromo-4-chloro-3-indolyl-β-D-galactopyranoside) at pH 6 to make a blue colored product [62]. X-gal is an organic compound consisting of an indole with a linked galactose. SA-β-gal seems to be associated with increased lysosomal mass of senescent cells [63]. Cells overexpressing p21 have a senescent phenotype and positive staining for senescence associated β-gal staining (Figure 1.11(b)) [51, 64, 65]. In HT1080 p21-9 cells, the senescent phenotype develops subsequently to cell growth arrest, starting at about 48 h

after the addition of IPTG (Figure 1.11(a)). Loss of clonogenicity is also observed after p21 overexpression and it correlates with the duration and level of p21 induction and is also linked to endoreduplication and abnormal mitosis after release from IPTG [48].

1.5 Cyclin Dependent Kinase 8 (CDK8) inhibitor Senexin A

Chemotherapy drugs which include the DNA damaging agents can induce tumor promoting paracrine activities in the vicinity of the tumor including the stromal region. These activities include promotion of tumor formation, stimulation of angiogenesis, metastasis, tumor resistance to chemotherapy, and secretion of multiple tumor-promoting cytokines [66-70]. Unlike the other members of the CDK family, CDK8 is an oncogenic protein which does not have any function in the cell cycle but is involved in many transcriptional programs related to carcinogenesis and the stem-cell phenotype [71, 72]. p21 has been shown to interact with CDK8 and its binding proteins namely, cyclin C and Med12 as indicated by immunoprecipitation assay in HT1080 p21-9 cells (Figure 1.12(a)). p21 has an opposite effect on the kinase activities of CDK2 and CDK8. As already known, it inhibits the CDK2 kinase activity, but in the case of CDK8, it has significant stimulatory effect (Figure 1.12(b)). Hence, p21 has a protective function against tumor which causes growth arrest in the cells through the inhibition of CDK2/cyclin E complex. On the other hand, p21 mediates chemotherapy induced tumor promoting paracrine activities by activating the CDK8/cyclin C complex (Figure 1.17)

Senexin A was developed by high throughput screening of >100,000 small molecules by monitoring the inhibitory effect on the p21 induced transcription, followed by chemical modification and optimization of the identified inhibitors. HT1080 p21-9 cells carrying a CMV-GFP construct were used as the tool for the high throughput screening. Initially 62 of the compounds tested showed a significant inhibition of p21 induced transcription as observed by the expression of GFP when normalized to the cell number and the protein content. Among these 62, a compound termed SNX2 and several other closely related compounds were found to be most effective. Subsequent steps of chemical derivatization and functional testing yielded a much more effective compound called Senexin A (Figure 1.13(b)). Senexin A belongs to the class of 4-aminoquinazolines (Figure 1.13(a)). Senexin A did not affect p21 expression (Figure 1.14(a)), or its activities including cell growth (Figure 1.14(b)), p21 induced senescent phenotype (Figure 1.14(c)) or p21 inhibitory effect on the expression of genes involved in cell cycle progression (Figure 1.15).

Senexin A selectively inhibits the kinases CDK8 and its isoform CDK19 as measured by ATP site-dependent competition binding assay [73] (Figure 1.16(a)). CDK8 acts as an oncogene in colon cancer through the β-catenin/Wnt pathway and Senexin A was found to inhibit the β-catenin regulated transcription [74, 75] as observed in the HCT116 colorectal carcinoma cells (Figure 1.16(b)). Other evidence of the effectiveness of Senexin A in inhibiting CDK8 is the inhibition of transcription factor EGR1 which gets activated in serum starved conditions [76] (Figure 1.16(c)).

1.6 DNA damaging effect of Doxorubicin

The DNA damaging agent doxorubicin introduces double stranded breaks in DNA by binding to topoisomerase II [77]. Double stranded breaks cause the activation of ATM kinases which phosphorylate p53. p21 is the important target of activated p53 which can lead to downstream interaction with CDKs to cause growth arrest. As mentioned earlier, accelerated senescence can be induced by DNA-damaging drugs [78]. Doxorubicin induces senescence effectively in a dose dependent manner (Figure 1.18(a)). In comparison to IPTG treatment of these same cells, doxorubicin is a stronger inducer of SA-β-Gal activity than IPTG if the level of p21 expression for each condition is considered. IPTG induces much higher levels of p21, yet the percentages of SA-β-gal positive cells do not exceed those of doxorubicin treated cells. Calculated levels of SA-β-Gal staining in doxorubicin treated cells normalized with the level of p21 is much less than the actual staining observed after doxorubicin treatment (Figure 1.18(b)).

Doxorubicin treatment induces growth arrest by 48 hours and it has a cytotoxic effect on HT1080 3'SS6 cells (Figure 1.19(a)). Doxorubicin treatment also gives rise to enlarged cells containing multiple completely or partially separated micronuclei with evenly stained chromatin which is a feature of mitotic cell death (Figure 1.19(b)).

In the present study, the dynamics of INoB formation in response to DNA damage by doxorubicin was assessed and its relation to various CDK inhibitors and rRNA transcription was analyzed to understand its function. HT1080 fibrosarcoma cell lines expressing CDK inhibitors such as p21, p16 and p27

provided a good model to study the nucleolar morphology without actually causing DNA damage. These cell lines were also helpful in studying the relationship between the senescent phenotype and INoBs. p21 interaction with CDK8 and its role in the nucleolar restructuring was facilitated by Senexin A which specifically inhibits CDK8 kinase activity. A major segment of the nucleolar function apart from ribogenesis is still unexplored. This study tries to unfold the structural dynamics and discover its relevance to the function of the nucleolus in stress response.

1.7 Aims of the current study

The current study was undertaken with the following aims:

1) Characterize the effect of CKIs and DNA damage and the effect of CDK8 inhibition by Senexin A on the formation of INoBs. This included the study of :
    a) INoB formation in response to different levels of p21
    b) INoB formation by overexpression of other CKIs such as p16 and p27 and the effect of CDK8 inhibition
    c) INoB formation by DNA damage and the involvement of p21 and CDK8.
2) Study of INoBs and other changes in the nucleolar structure associated with some aspects of the senescent phenotype. This included the study of:
    a) INoB formation at quiescent stage as compared to senescent cells.
    b) INoBs and other nucleolar changes associated with transcription-related changes of senescent cells (RNA polymerase I and II).

c) senescent phenotype (SA-β-gal, increased cell size and granularity) associated with the formation of INoBs and the effect of CDK8 inhibitor.

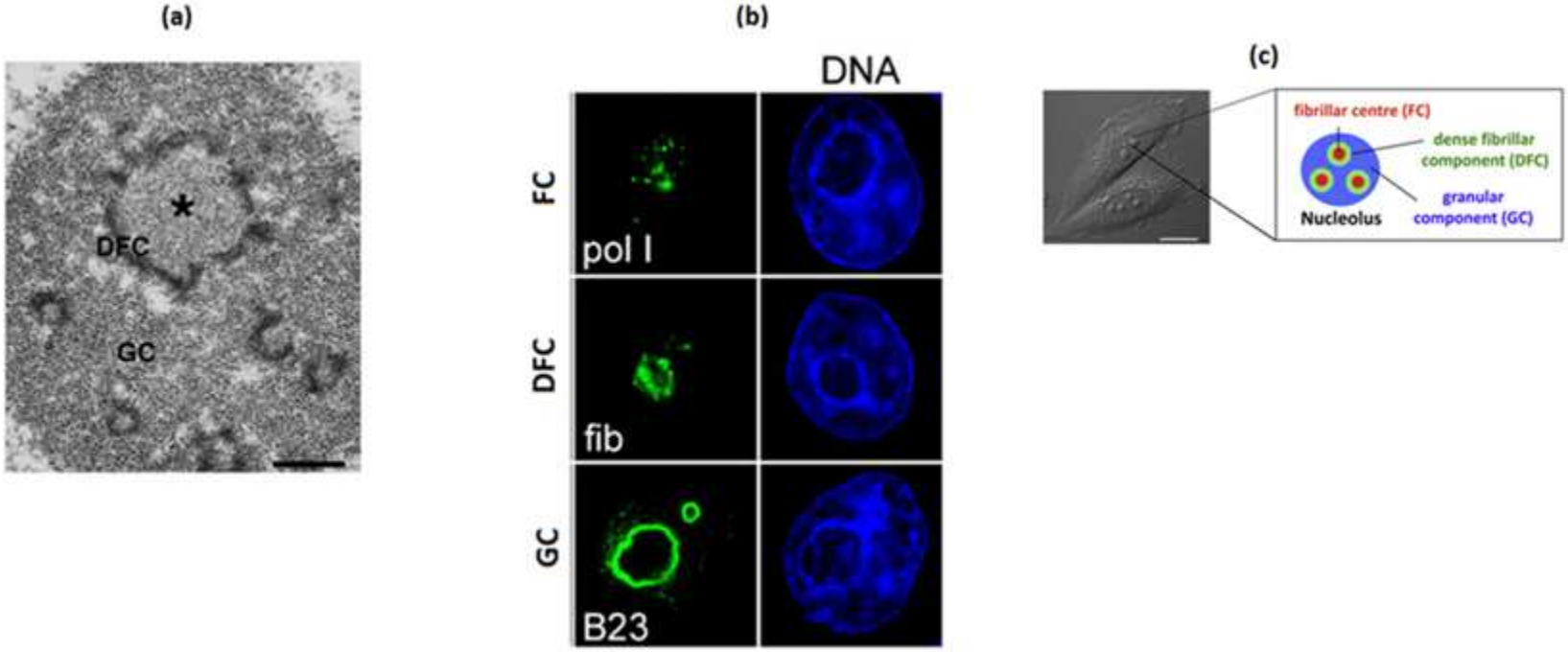

Figure 1.1 Structure of nucleolus. (a) A Nucleolus as seen by electron microscopy in HeLa cells showing the three compartments; Fibrillar center (FC) marked by the asterisk, Dense fibrillar component (DFC) and Granular Component (GC). Bar, 0.5 µm [79]. (b) HeLa cells stained by specific antibodies for RNA polymerase I (pol I), fibrillarin (fib) or B23 as marker proteins for the FC, DFC or GC, respectively (Left panel). Right panel showing the DAPI staining for the same cells [28]. (c) Schematic representation of FC, DFC and GC region in the nucleolus of the live HeLa cells. Bar, 15 µm [10]

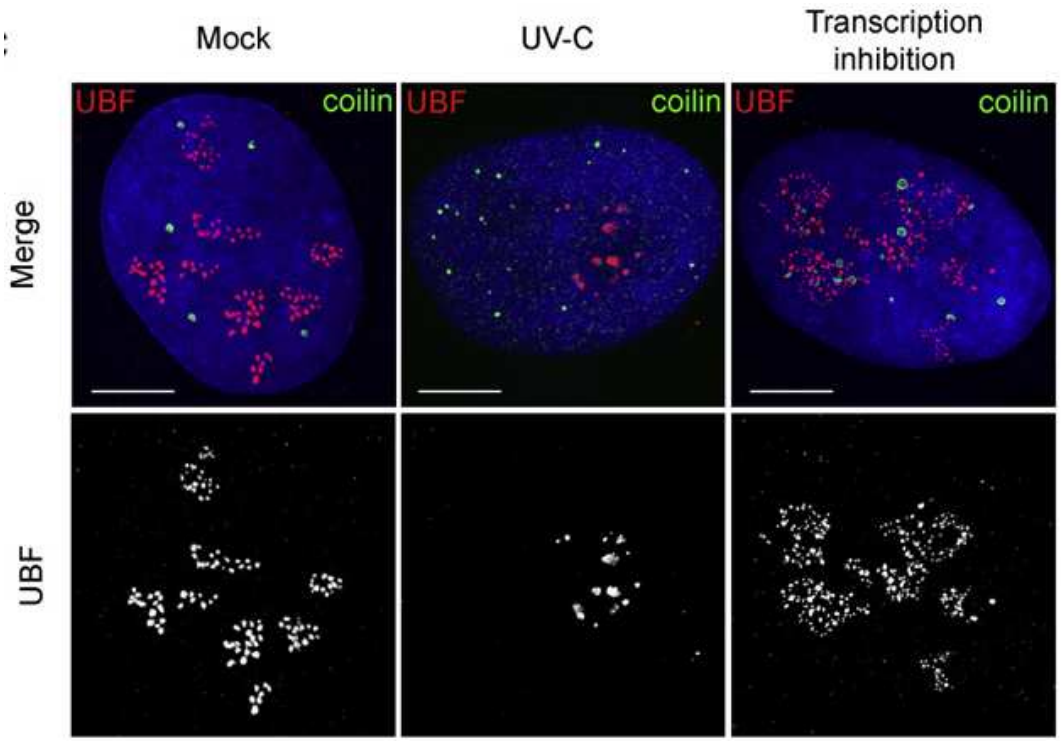

Figure 1.2 Stress induced changes in the nucleolus of U2OS cells. Untreated cells (left panel), UV-C (6 h post irradiation, 30J/m^2) treated (middle panel) and DRB (3 h treatment, 25 µg/ml) treated (right panel) stained for upstream binding factor (UBF) showing FC region in red and coilin in green. UV-C treatment is showing nucleolar segregation while DRB treatment causes nucleolar disruption. Bar, 5 µm.[10]

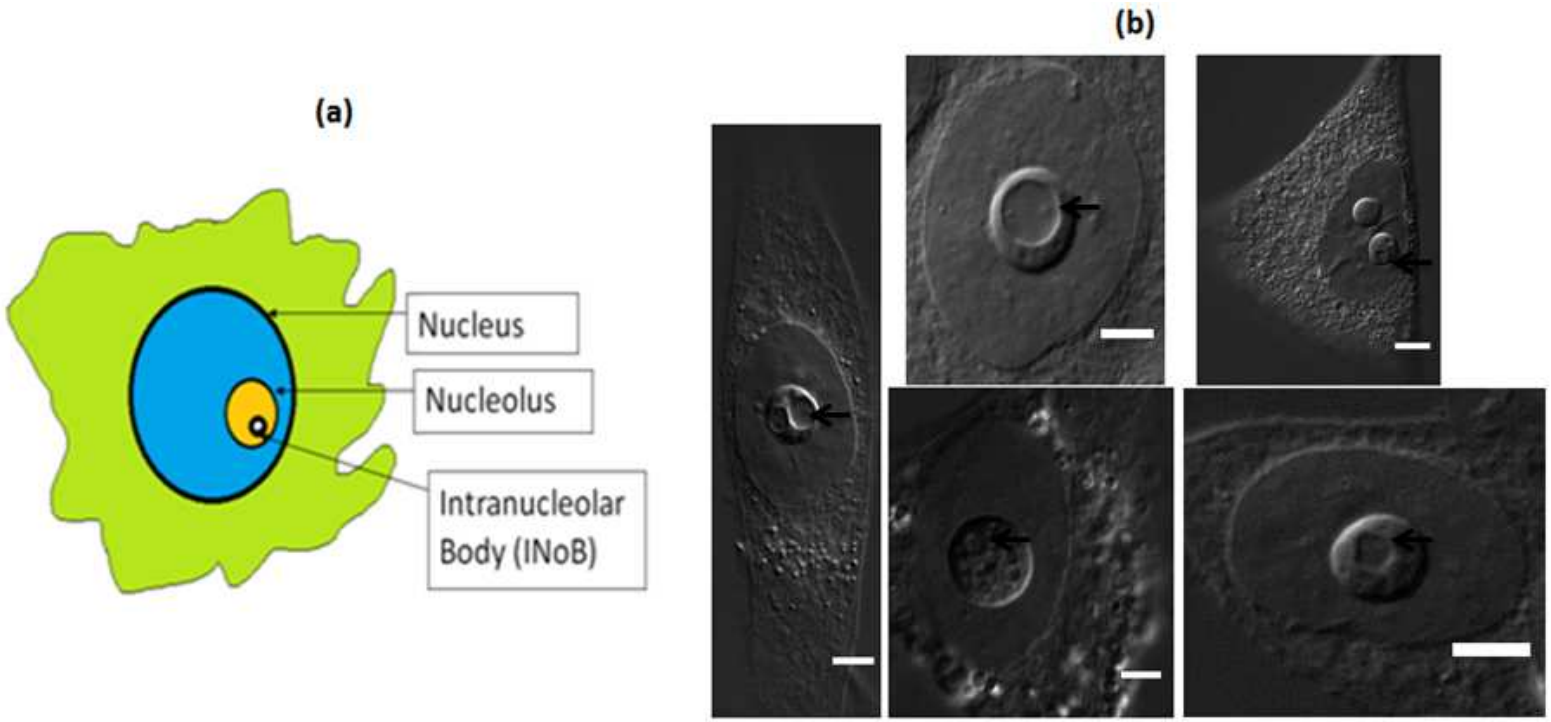

Figure 1.3 Intranucleolar Body. (a) A schematic diagram showing the relative positions of nucleus, nucleolus and intranucleolar body (INoB) in a cancer cell. (b) HCT116 colorectal cancer cells treated with 160nM DNA-damaging agent doxorubicin for 48 hours showing the formation of INoBs (indicated by the arrows). Bars, 5 µm

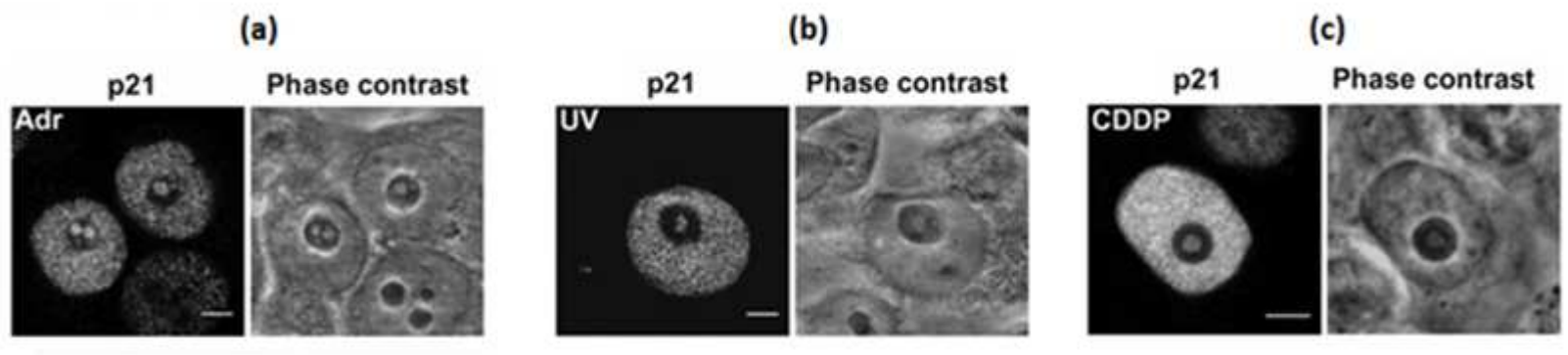

Figure 1.4 p21 localization in INoBs after DNA damage. (a) HCT116 cells treated with 258 nM doxorubicin (Adr) for 48 hours (b) Same cells exposed to 30 J/m^2 UV rays and analyzed after 24 hours (c) The same cells treated with 10 µM cisplatin (CDPP) for 24 hours. Left panel showing the immunostained cells for p21 while the right panel showing the phase contrast images. Bars, 5 µm [27].

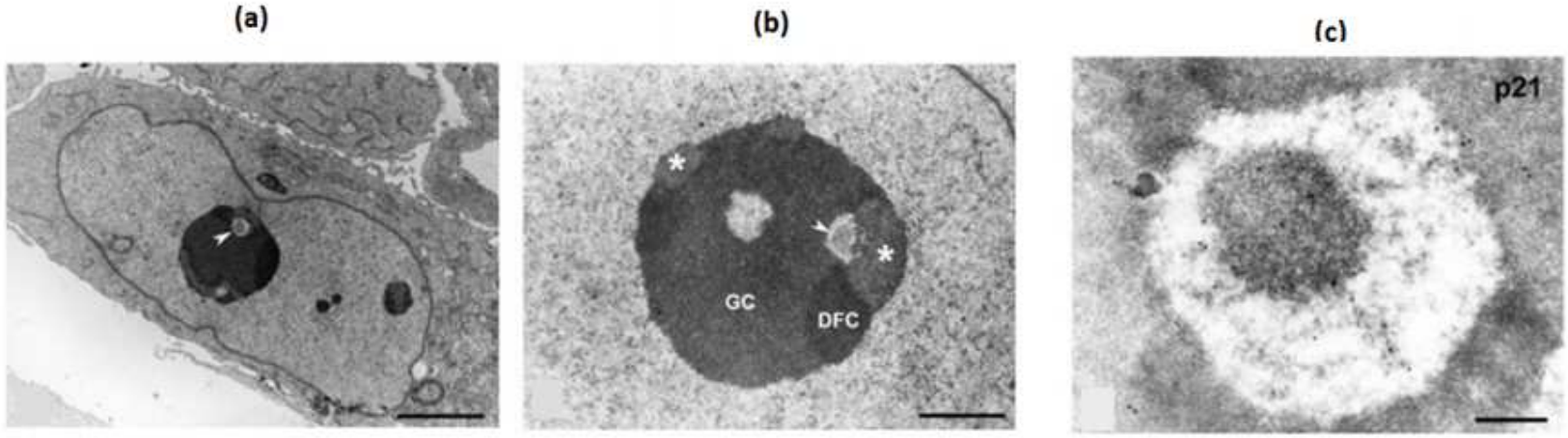

Figure 1.5 Electron micrographs showing INoBs. (a) Electron micrograph of HCT116 cell treated with doxorubicin for 24 hours show the formation of INoB (indicated by arrowhead) inside the nucleolus. (b) HCT116 cell treated with doxorubicin shows the formation of INoBs (indicated by arrowhead) and other compartments of nucleolus: fibrillar center (FC), dense fibrillar component (DFC) and granular component (GC). (c) A magnified image of the nucleolus by immunogold electron microscopy of p21 in doxorubicin treated cells showing the localization of p21 in the INoBs (black dots). Bars (a) = 3um, (b) = 1um and (c) = 350nm [27].

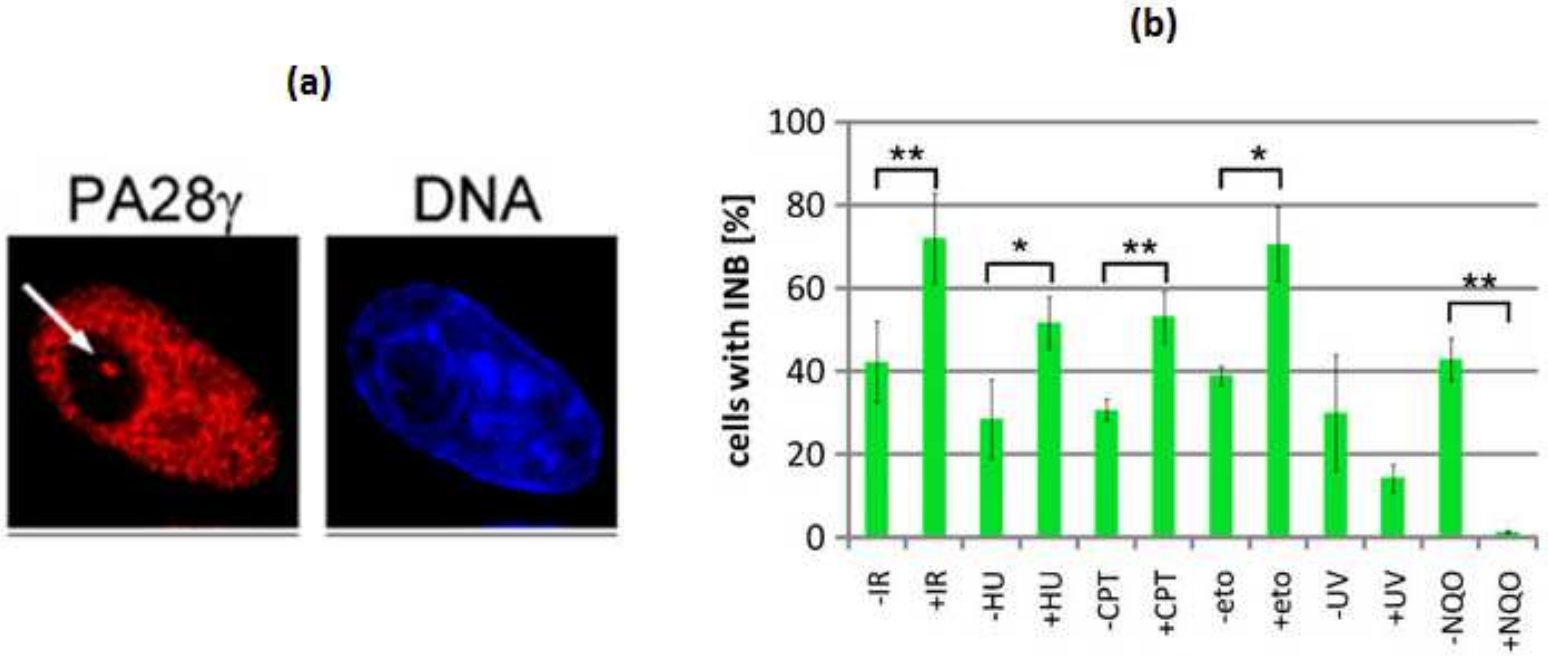

Figure 1.6 Effects of DNA damage on Intranucleolar body (INB). (a) An untreated HeLa cell showing the presence of INB (indicated by arrow). INBs were labeled with antibodies against the endogenous PA28γ (b) Graph showing the changes in the frequency of HeLa cells having INBs when treated with different DNA damaging agents: Ionizing radiation (IR), Hydroxyurea (HU), Camptothecin (CPT), Etoposide (eto), UV radiation (UV) and an UV mimetic 4-Nitroquinoline 1-oxide (NQO). p-values were determined using a heteroscedastic, two-tailed t test and are indicated as singleasterisk for p≤0.05 (significant) and double asterisk for p≤0.01 (highly significant) [28].

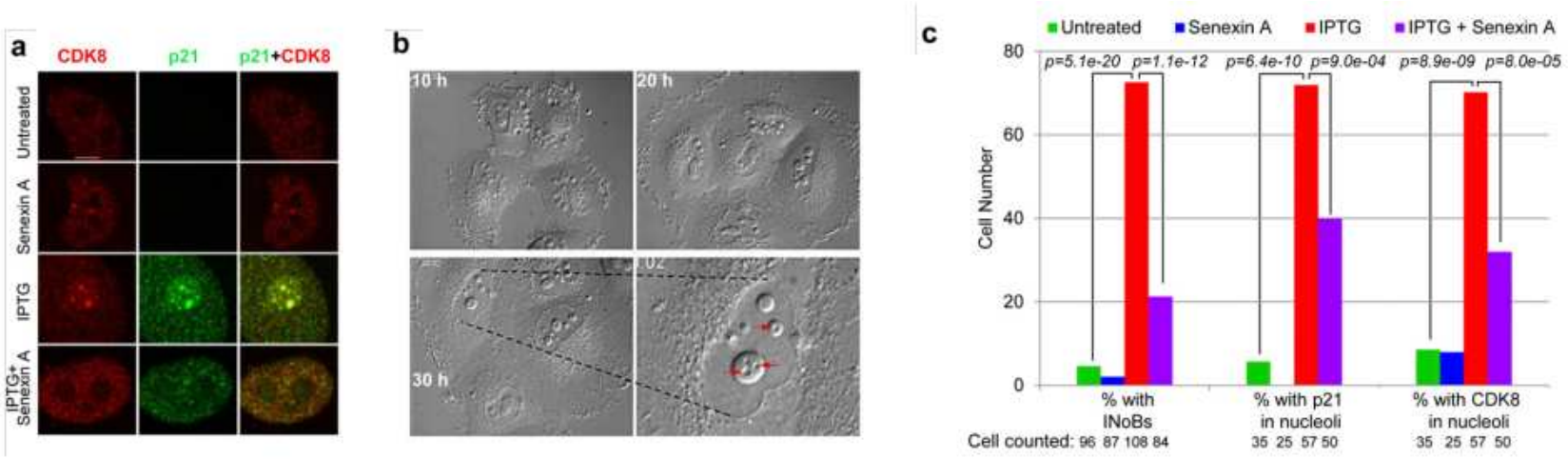

Figure 1.7 Initial studies of INoBs in our laboratory. (a) HT1080 p21-9 cells treated with 50 µM IPTG with or without 10 µM Senexin A for 48 hours and then immunostained for p21 (green) and CDK8 (red). (b) Time lapse microscopy shows the formation of INoBs in HT1080 p21-9 cells after p21 induction by 50 µM IPTG. INoBs are indicated by arrows. (c) HT1080 p21-9 cells treated with 50 µM IPTG with or without 10 µM Senexin A and then scored for the presence of INoBs and the localization of p21 and CDK8 in the nucleoli. Numbers of cells scored are shown. A chi-square test was used to measure the statistical significance. p-value<0.05 (*) [29]

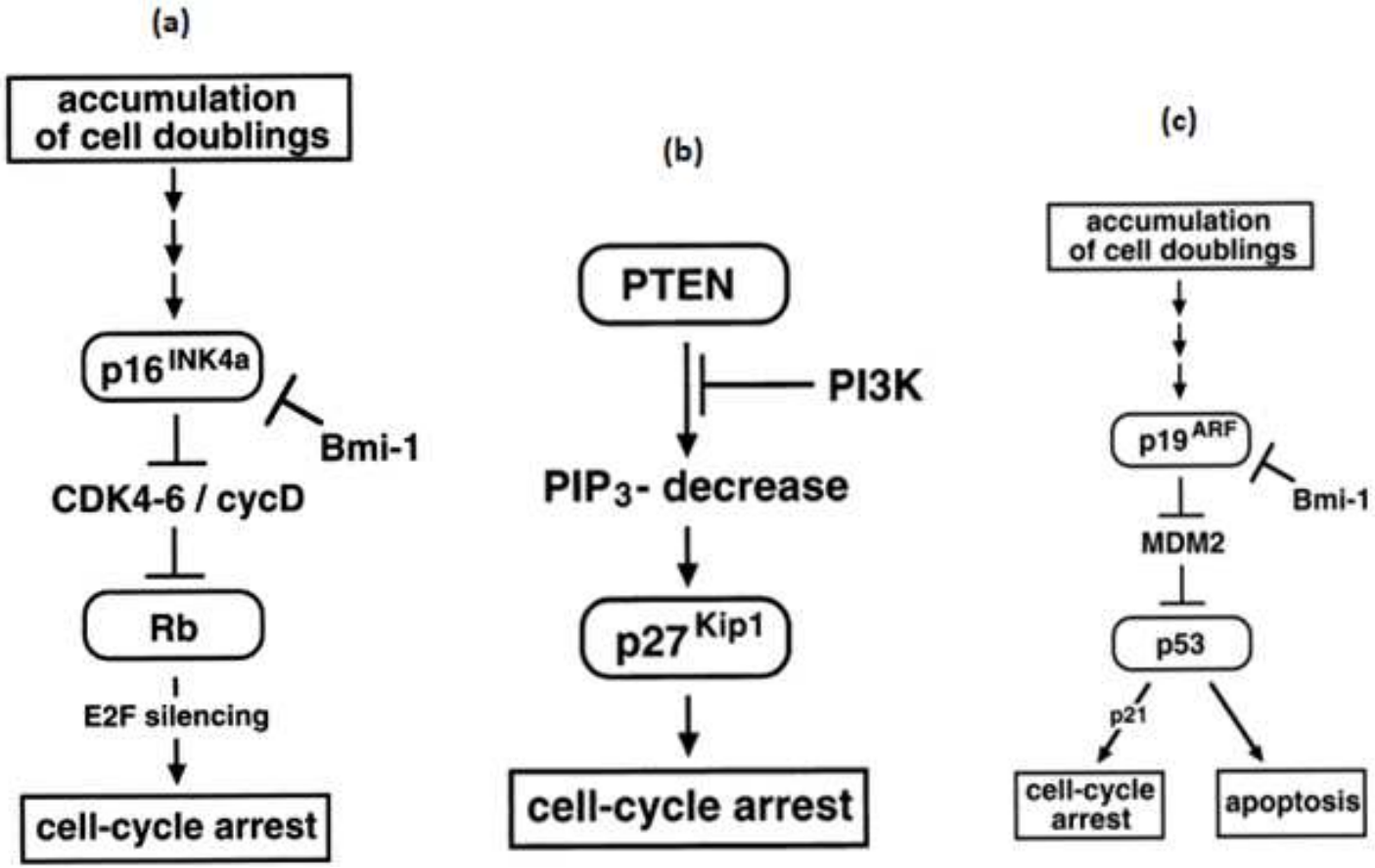

Figure 1.8 Different pathways of growth arrest and apoptosis by CDK inhibitors.
(a) The p16/Rb pathway for growth arrest in dividing cells.
(b) PTEN/p27 pathway showing the relevance of p27 in the cell cycle growth arrest.
(c) Involvement of p53 and p21 in the process of cell cycle arrest. [80]

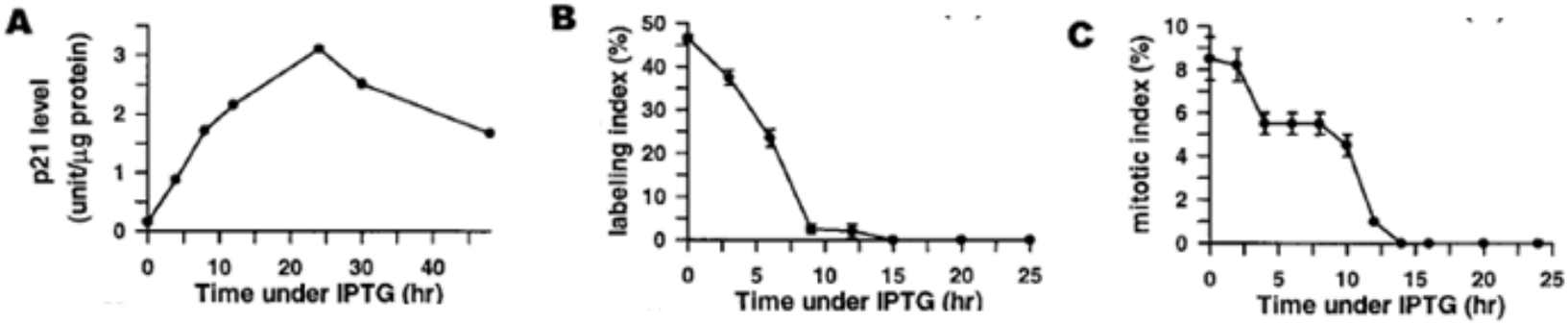

Figure 1.9 p21 overexpression in HT1080 p21-9 cells. (a) A time course analysis of p21 levels after the addition of 50 μM IPTG in HT1080p21-9 cells over 48 hours. p21 levels were determined by using the waf1 ELISA kit. (b) Time course analysis of thymidine [^{3}H] labeling index after the addition of 50 μM IPTG determined by autoradiography. (c) Time course analysis of mitotic index after the addition of 50 μM IPTG as determined by 4',6-diamidino-2-phenylindole (DAPI) staining [53].

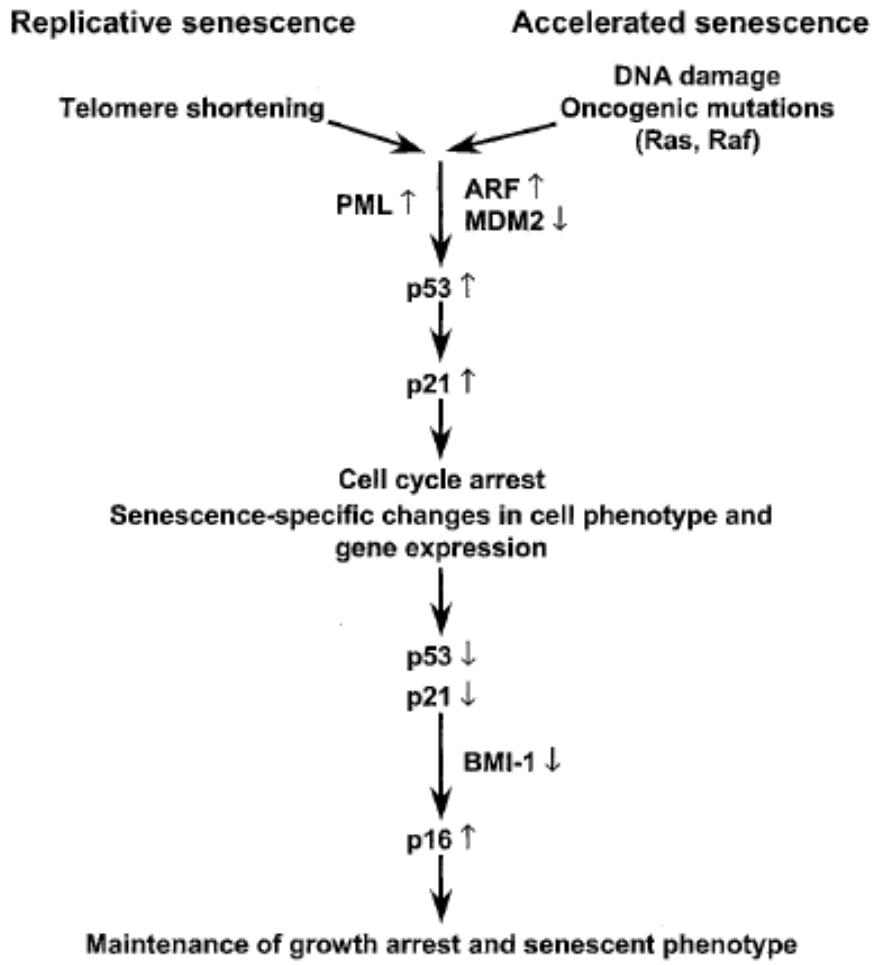

Figure 1.10 Pathways involved in the growth arrest during senescence process [81].

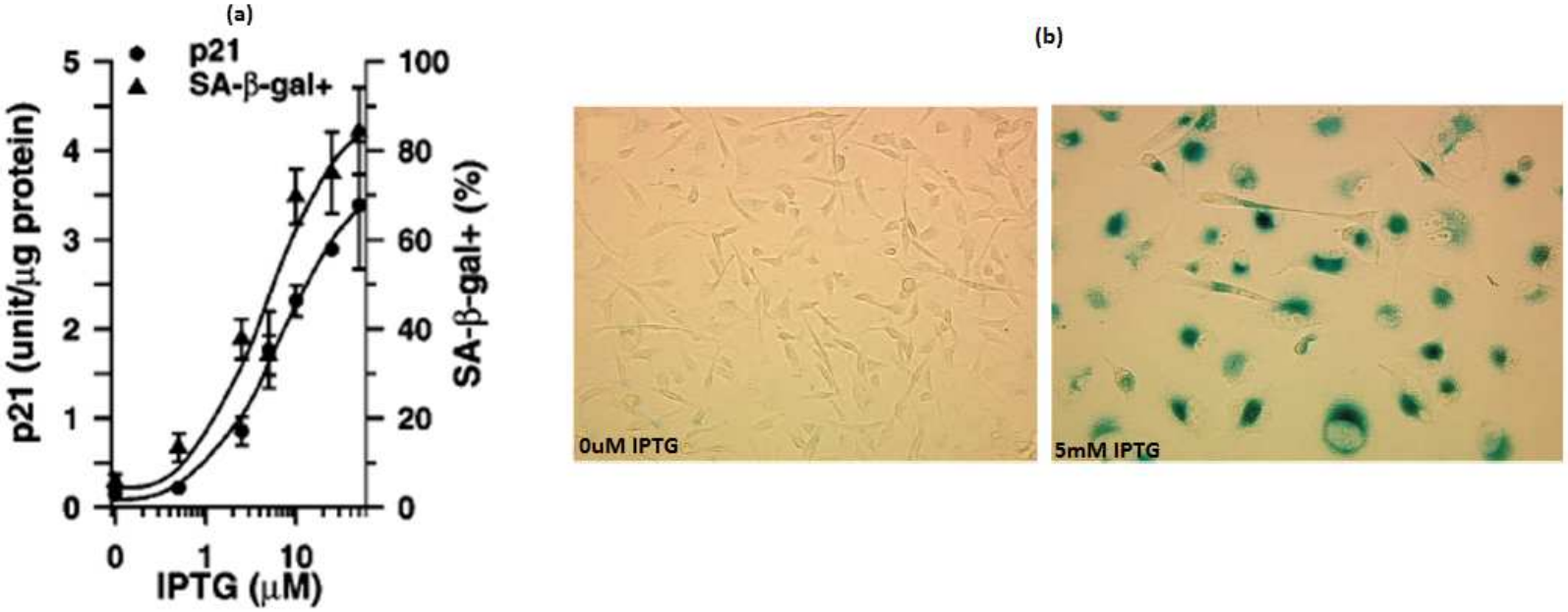

Figure 1.11 IPTG induced senescence in HT1080 p21-9 cells. (a) Dose-dependent induction of p21 protein and SA-β-gal staining in HT1080 p21-9 cells by 48 h exposure to IPTG. p21 levels were determined by ELISA. (b) SA β-Gal staining of HT1080 p21-9 cells treated with 5 mM IPTG for 4 days [51].

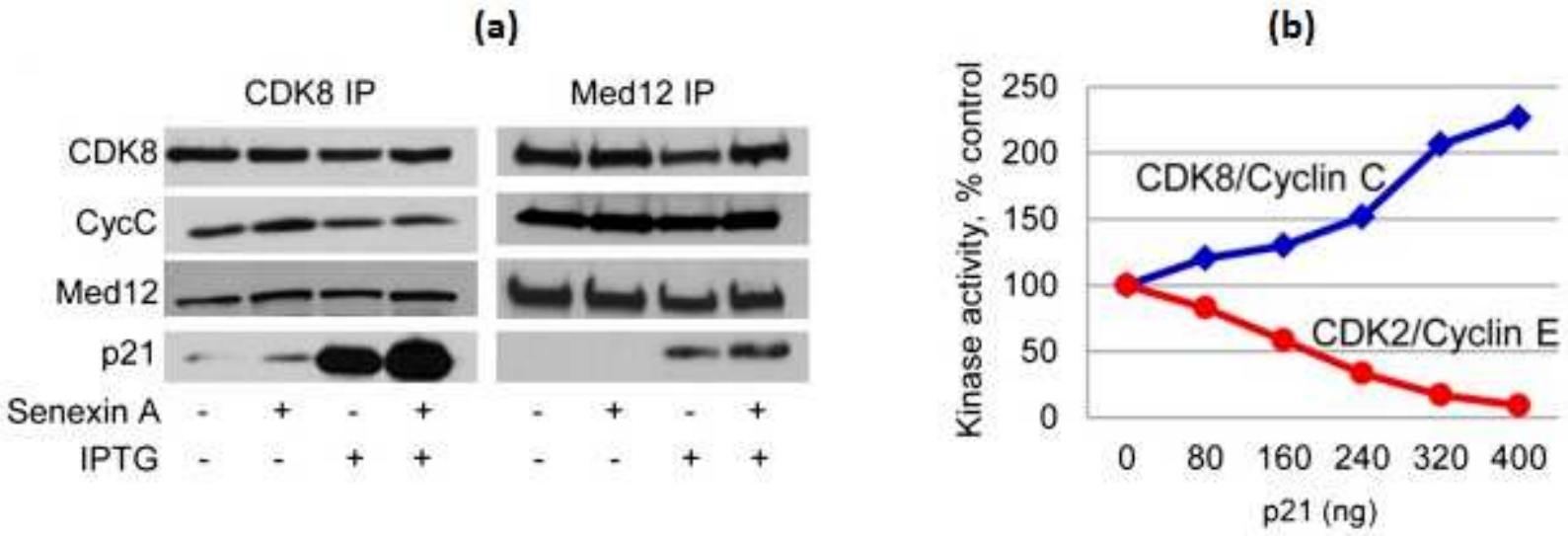

Figure 1.12 Interaction of p21 with CDK8. (a) HT1080 p21-9 cells were treated with 10 μM Senexin A with and without 50 μM IPTG for 48 hours and then analyzed by immunoprecipitation of CDK8, Med12, cyclin C, and p21 (b) Graph depicting the opposite effects of recombinant p21 on CDK2/cyclin E and CDK8/cyclin C kinase activities in cell free assays [29].

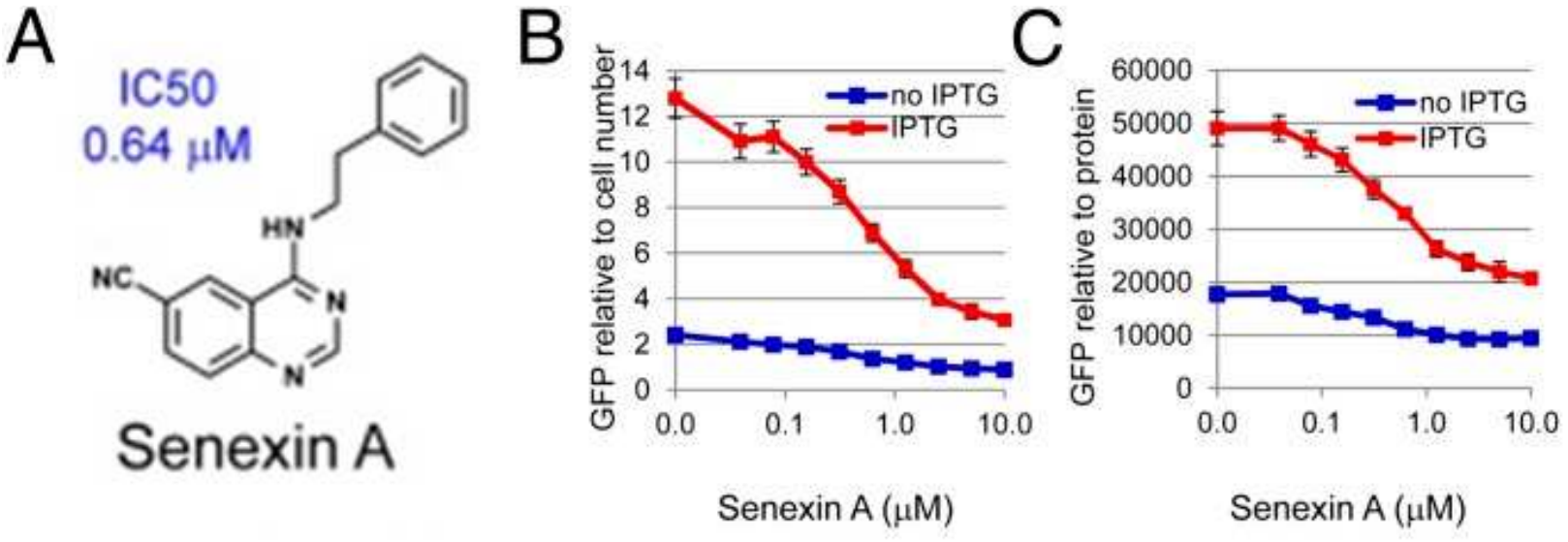

Figure1.13 Effects of Senexin A. (a) Structure of Senexin A. (b) HT1080-p21-9 cells were treated with 50 µM IPTG for 48 h (quadruplicate assays) and CMV-GFP expression was measured and normalized to Hoechst 3342 DNA staining which is a measure of relative cell number. (c) Same as in B, except that GFP fluorescence was normalized by sulphorhodamine B staining (a measure of protein amount) [29].

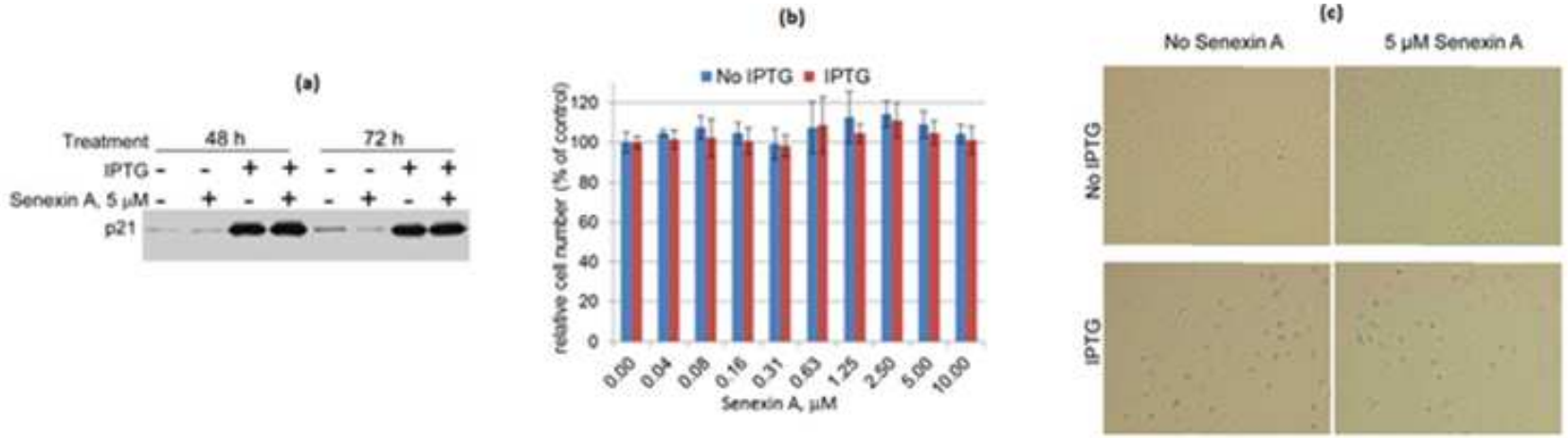

Figure 1.14 (a) Western blot showing the expression of p21 in HT1080 p21-9 cells after 50 µM IPTG treatment with or without 5 µM Senexin A for 48 h and 72 h (b) Graph showing the relative cell numbers (as measured by Hoechst 33342 fluorescence) after 72 hours treatment with different concentrations of Senexin A with or without 50 µM IPTG (c) HT1080 p21-9 cells treated with 50 µM IPTG with and without 5 µM Senexin A and then stained for SA-β-Gal [29].

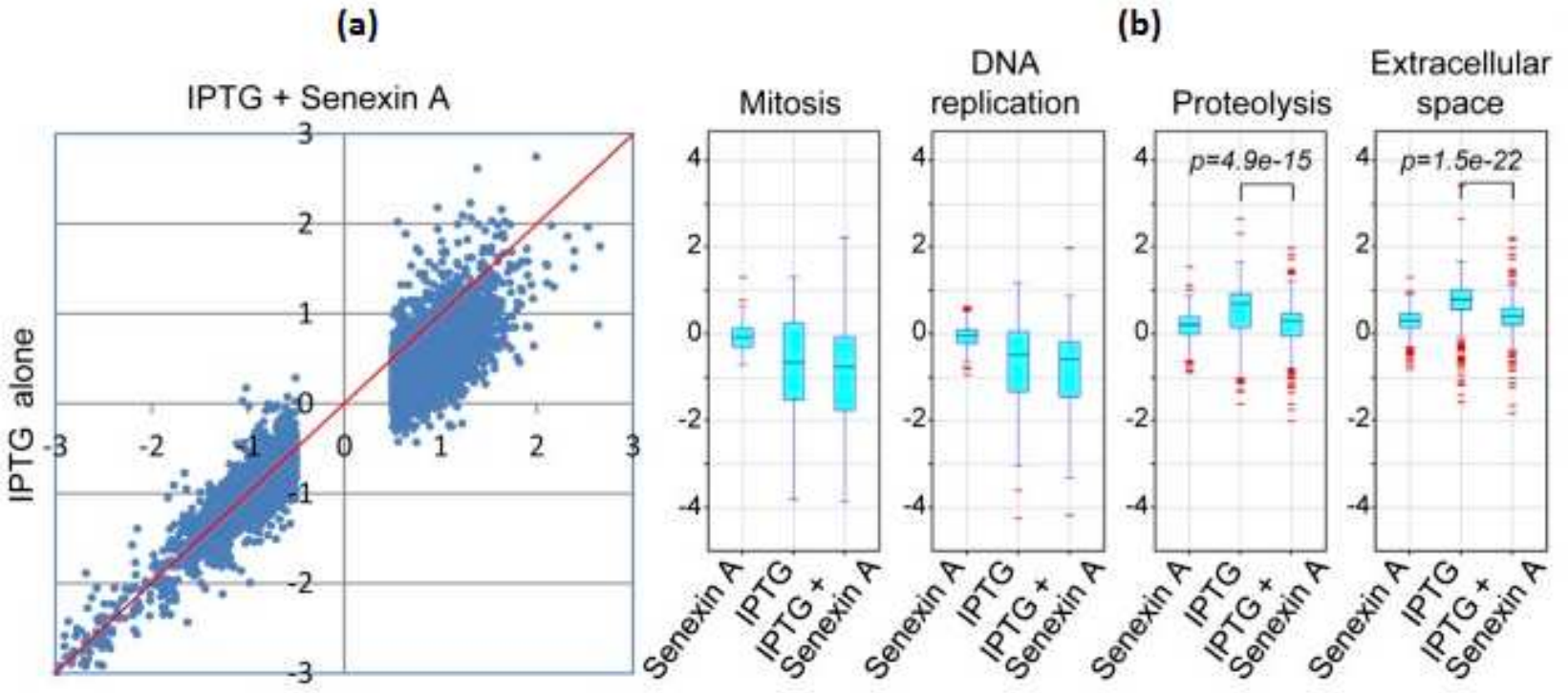

Figure 1.15 Senexin A does not affects p21 inhibitory effects. (a) Microarray data of HT1080 p21-9 cells treated with only 50 μM IPTG (x axis) or with 50 μM IPTG and 5 μM Senexin A (y axis) for 48 h. Fold changes in gene expression are plotted as log2; genes showing IPTG-induced fold changes with log2 < 0.5 are excluded.
(b) HT1080 p21-9 cells were treated with Senexin A, IPTG, or IPTG plus Senexin A and gene expression according to the Gene Ontology (GO) categories is represented by using Box-whisker plots showing fold changes for all the genes in that category [29].

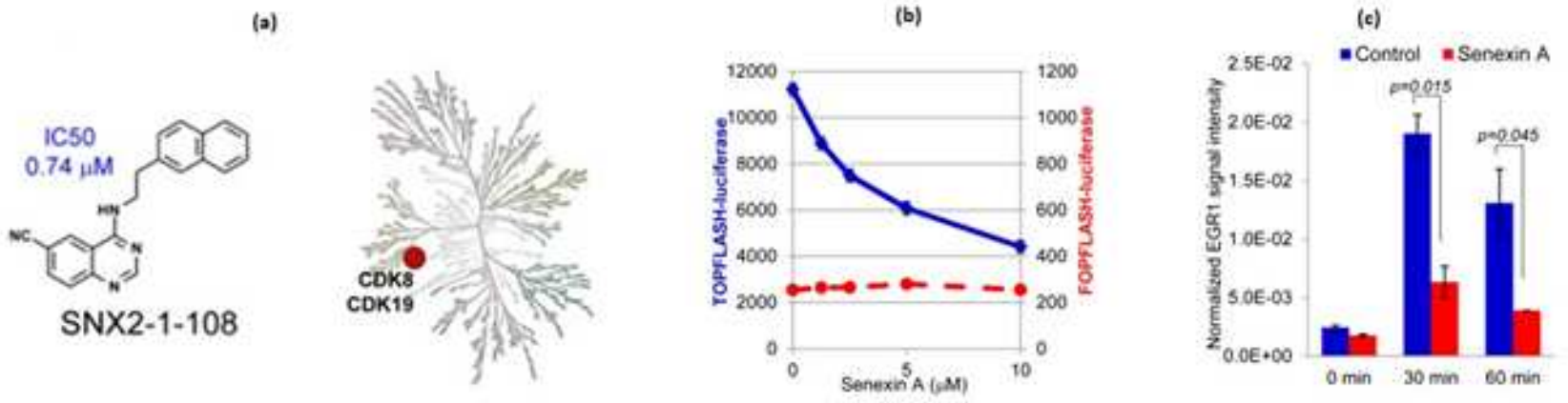

Figure 1.16 Senexin A inhibits CDK8/CDK19. (a) Effects of 2 μM Senexin2-1-108 which is an analogue of Senexin A on the activity of 442 kinases, measured by ATP binding competition assay. The dendrogram of the kinases with the inhibited kinases (CDK8 and CDK19) are shown by the red dots. (b) HCT116 cells were treated with different concentrations of Senexin A and luciferase expression from β-catenin–dependent promoter (TOPflash) or its β-catenin–independent version (FOPflash) was measured after 48 hours treatment. (c) HT1080 p21-9 cells were serum starved for 48 h, followed by re-addition of serum for the indicated periods of time, in the presence or absence of 5 μM Senexin A and then quantitative PCR analysis was performed for EGR1 mRNA expression [29].

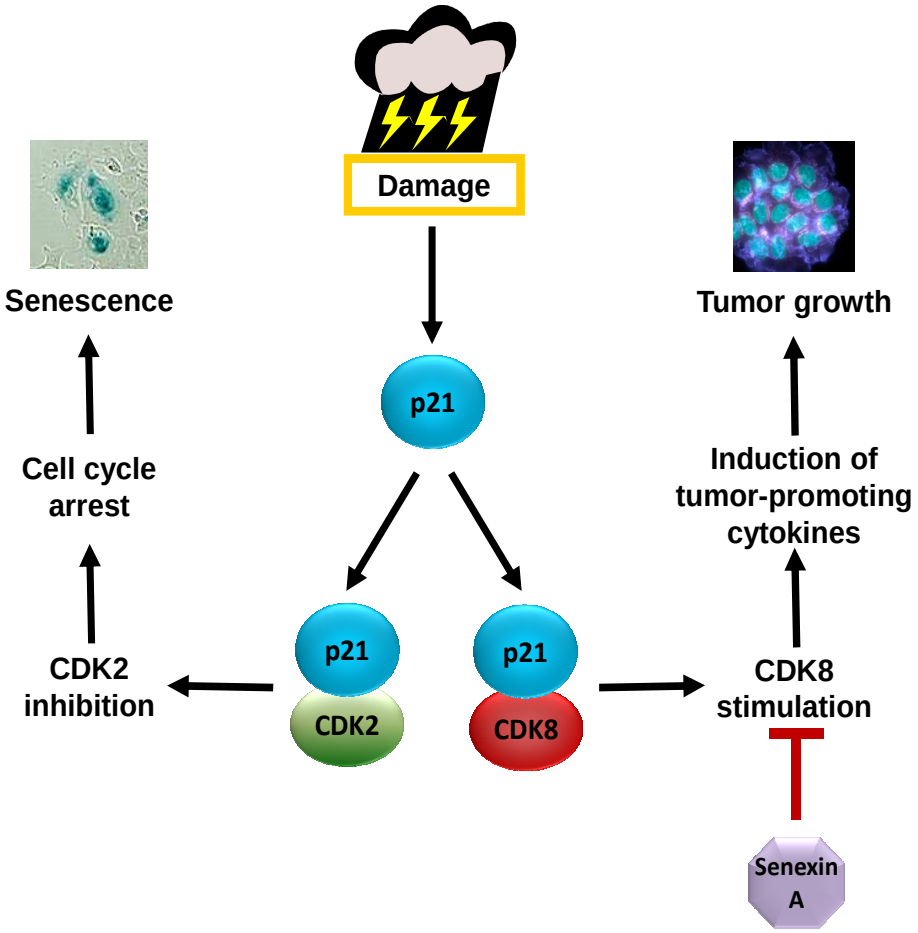

Figure 1.17 Alternate pathways showing the role of p21 under the effect of DNA damage and the effect of Senexin A [29].

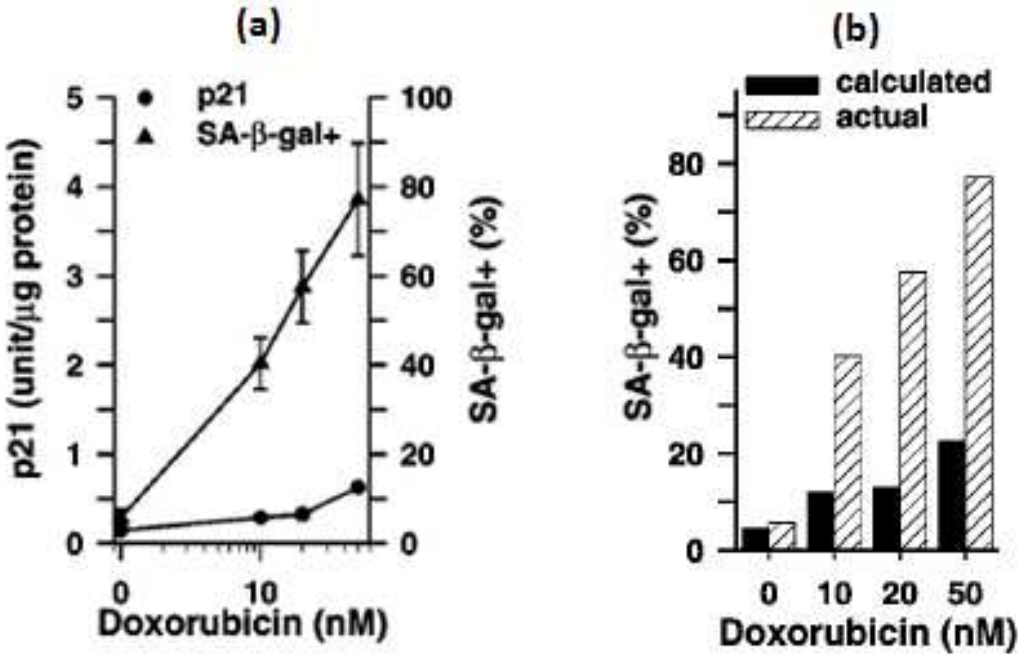

Figure 1.18 Doxorubicin induced cell senescence. (a) HT1080 p21-9 cells treated with different concentrations of doxorubicin for 48 hours show the dose dependent relationship between concentration and induction of p21 and SA-β-Gal positive (senescent) cells. (b) Induction of senescence normalized to p21 levels by doxorubicin as compared to IPTG in HT1080 p21-9 is indicated in the graph (see Figure 1.11) [51].

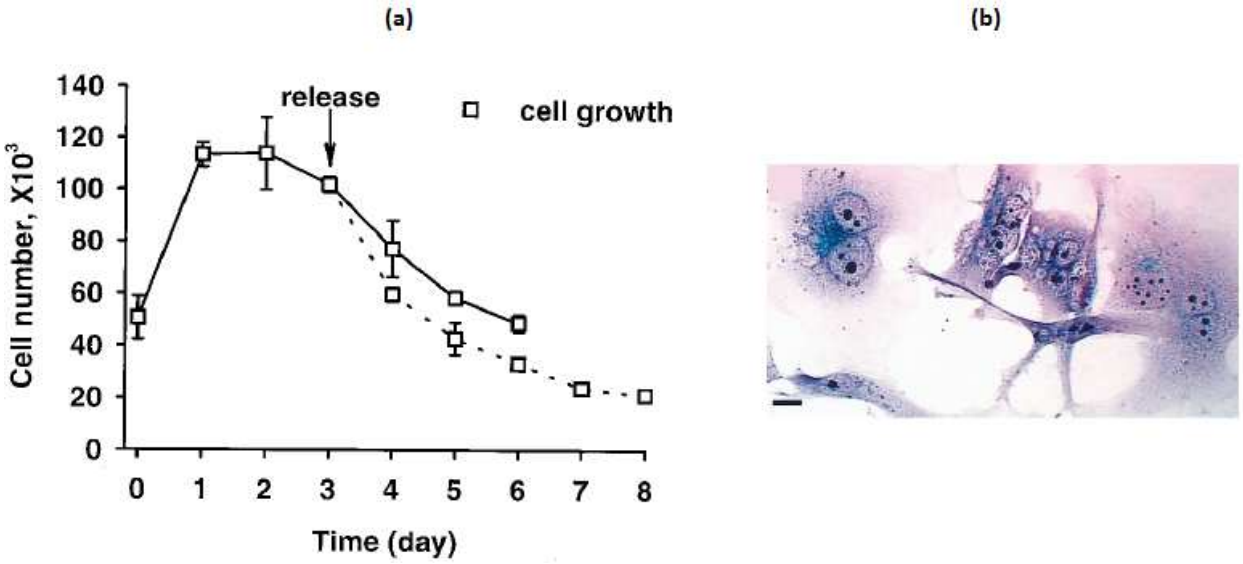

Figure 1.19 Effect of doxorubicin on cell growth. (a) HT1080 3'SS6 cells were treated with 30 nM doxorubicin either continuously (solid lines) or release after 3 days (dashed lines) and cell growth was measured using methylene blue staining.
(b) HT1080 3'SS6 cells treated with 30 nM doxorubicin for 72 hours and then stained for SA-β-Gal and H & E (Hematoxylin and Eosin).

CHAPTER 2

MATERIALS AND METHODS

2.1 Cell lines

Different cancer cell lines were used in this study. HCT116 wild-type and p21-/- (clone 80S4) [82, 83] were a gift of Dr. B. Vogelstein (Johns Hopkins University). HT1080 subline 3'SS6 was derived after transfection with the murine ecotropic retrovirus receptor and Lac I repressor genes as previously described [52]. HT1080 p21-9, HT1080 p16-5 and HT1080 p27-2 cell lines were used which have an IPTG inducible p21, p16 and p27 genes, respectively. All the cells were grown in DMEM/High glucose medium (HyClone) with 10% FCII serum (Hyclone). 1% penicillin (100 units/ml), 1% streptomycin (292 µg/ml) and glutamine (2 mM) were also added to the growth medium. A standard cell culture regime was used to culture the cells and cultures which were 70-80% confluent were used for the experiments. Cell lines were maintained in culture for around 10-15 passages (one passage in 3-4 days). In most cases, 20-80 cells per square millimeter of culture dish were used as a standard cell density for the passage.

2.2 Drug and IPTG treatment

Doxorubicin was used for the damage-inducing treatment and according to the experiment different concentrations were used for different time periods. IPTG (Isopropyl β-D-1-thiogalactopyranoside) at 50 µM final concentration was used to induce expression of p21 in HT1080 p21-9, or p16 or p27 in the 16-5 or p27-2 fibrosarcoma cell lines. Similar IPTG concentration was used for the induction of p16 and p27 in HT1080 p16-5 and HT1080 p27-2 cell lines. Senexin A which is a CDK8 inhibitor developed in our laboratory through high throughput screening and chemical optimization of small molecules was used at 5 µM final concentration in all the experiments [29]. Equal volumes of dimethyl sulfoxide were used in place of Senexin A stock in control samples. Usually the cells were seeded for the experiment on day 1 and treatment was performed the next morning after the cells had attached to the culture plate.

2.3 Immunocytochemistry

Cells were seeded on glass coverslips in 6-well plates. After the treatment, cells were fixed with 4% paraformaldehyde in 0.1 M mixed phosphates buffer solution (20 minutes treatment). Sodium dihydrogen phosphate (0.2 M) and disodium hydrogen phosphate (0.2 M) were mixed in 1:4 ratios to prepare 0.2 M mixed phosphate buffer solution. For the permeabilization of the cells, a five minute 0.5% triton X wash was performed followed by two PBS washes of five minute intervals. Then the coverslips were transferred into the humid chamber where a block solution (100 µL) was added for 40 to 60 minutes time. The block was performed by using 3% Normal Donkey serum (NDS)/1% Bovine serum

albumin (BSA)/0.02% Sodium azide in PBS. According to the protein being probed the primary antibodies were added with required dilutions in 1%BSA/0.02% Sodium azide in PBS solution. Primary antisera used were mouse anti-p16 (Oncogene, cat#NA29, 1:100); goat anti-CDK8 (SantaCruz, cat#sc1521, 1:400); mouse anti-fibrillarin (Encore, cat#MCA38F3) and mouse anti-RNA polymerase I (SantaCruz, cat#sc48385, 1:1000). The coverslips were incubated overnight in 100 µL of the primary antibody solution at 4^{o} C. The next day, again a 5 minute wash was done using 0.1% triton X solution followed by two PBS washes of 5 minute interval. Again the coverslips were transferred into the humid chamber. A block solution (100 µL) of 1%BSA/0.02% sodium azide in PBS was used for blocking (40-60 minutes). After the blocking, secondary antibodies according to the origin of the primary antibodies were diluted in blocking solution. Secondary antibody solution (100 µL) was added on the coverslips for an hour. A wash of 5 minutes was done by 0.1% triton X solution followed by two PBS washes. At this point, DAPI (4′,6-diamidino-2-phenylindole) staining of the cells was done which stains the DNA. The DAPI stain with 1:10000 dilution in PBS was added for 10 minutes. After two more PBS washes (5 minutes), coverslips were ready to be mounted. Coverslips were mounted on the slides by using the mounting solution (50% glycerol/0.02% sodium azide in PBS). Immunostained cells on the slides were observed on an Olympus IX81 fluorescent microscope.

2.4 Intranucleolar Body and RNA polymerase aggregate scoring

An Olympus IX81 fluorescent microscope was used for the scoring of cells for the presence of INoBs and Pol I aggregates. Blind scoring was performed for all the experiments and according to the experiments 50-200 cells per condition were counted by using this method.

For the INoB scoring, the slide was mounted, and the cells were observed using a 60x/1.4 n.a objective with differential Interference contrast (DIC) optics. The live image from the Hammamatsu camera was directed to the computer monitor. A random field was selected on the coverslip area and then only the cells with clear and observable nucleus within that field were considered for the scoring. Focus was adjusted according to the best visible INoB in the nucleolus. Cells having even a single INoB were considered positive. Some cells have multiple nucleoli; in that case, presence of an INoB in any nucleolus was considered as positive. This was repeated for all the cells in different fields of the coverslip. The stage was moved in an orderly direction so that overlapping fields were not selected.

For Pol I aggregate scoring, the GFP fluorescence filter set was used for imaging RNA polymerase I indirectly labeled with AlexaFluor488. Similar to the INoB scoring, random fields were selected and for each observable cell focus was adjusted to see a bright circular spot visible inside the nucleolus. Cells were scored positive if they had this peculiar staining pattern for the RNA polymerase I.

2.5 Senescent associated β-Galactosidase (SA β-Gal) staining

SA β-Gal staining detects the presence of the enzyme β-galactosidase in the senescent cells by its digestive activity on the organic substrate 5-bromo-4-chloro-3-indolyl-β-D-galactopyranoside (X-Gal) which gives rise to a blue colored product observable under the microscope. After the required treatment according to the experiment, the cells were fixed by using the fixing solution which consists of 2% formaldehyde and 0.2% gluteraldehyde in phosphate buffered saline (PBS). After removing the growth media from the cells, they were washed twice with PBS (2 ml/well) and then the fixing solution (2 ml/well) was added. After 10 minutes, cells were again washed twice with PBS (2 ml/well) and staining solution (2 ml/well) was added. Staining solution consists of 8% Disodium phosphate (0.5 M) with pH=6 adjusted by citric acid, 10% pottassium ferricyanide (50 mM), 10% pottassium hexacyanoferrate (II) (50 mM), 3% sodium chloride (5 M), 0.2% magnesium chloride hexahydrate (1 M), 5% 5-bromo-4-chloro-3-indolyl-β-D-galactopyranoside (X-gal) in double distilled (dd) water. After incubation in staining solution at 37^{o} C for 24-30 hours, the cells were observed under a Leica DMIRE2 microscope for the presence of blue color in the cytoplasm which characterize them as senescent.

2.6 Western blots

Western blotting was carried out on the nucleolar extracts obtained from Dr.Dmitri Pestov's lab (University of Medicine and Dentistry of New Jersey). The nucleolar lysates were diluted in the nucleolar extract buffer (NE buffer). The nucleolar extract buffer consisted of 50 mM Tris-HCl, pH 7.6; 150 mM NaCl; 1

mM EDTA; 0.5 mM EGTA; 0.1% SDS and 1 mM Dithiothreitol (DTT). We used 10 µg of the nucleolar extracts per well for loading. Loading buffer used for gel electrophoresis consisted of 250 mM Tris-HCl, pH 6.8; 40% Glycerol; 5% SDS; 0.025% Bromophenol blue and 10% β-mercaptoethanol in dd water. BioRad Mini Protean TGX Gradient gel (4-15%) was used for the electrophoresis. Wet transfer method was used to transfer the proteins from gel onto the PVDF (polyvinylidene difluoride) membrane. After the transfer the PVDF membrane was blocked by immersing it in 5% non-fat dry milk for 1 hour with gentle shaking. The primary antibodies were diluted in 5% non-fat dry milk and the PVDF membrane was incubated overnight in it at 4^{o} C. We used the primary antibodies goat anti-CDK8 (Santacruz, cat#sc1521, 1:800), mouse anti RNA polymerase II (AbCam, cat#ab5408, 1:1000), mouse anti-RNA polymerase I (Santacruz, cat#sc48385, 1:1000), mouse anti-fibrillarin (Encore, cat#MCA38F3, 1:1000) and anti-p21 (Calbiochem, cat#OP64, 1:1000). Next day, the membrane was washed with 1X TBST buffer which consists of 50 mM Tris-Base, 60 mM KCl, 2.8 M NaCl and 1% Tween-20 in dd water. Then the corresponding horse radish peroxidase labeled secondary antibodies (1:5000) diluted in 5% non-fat dry milk were added for 1 hour with constant shaking. After 1 hour, membrane was washed with 1X TBST and X-ray film is developed by using the Perkin-Elmer (Western lightning- plus ECL) chemiluminescence kit. Fiji software was used for doing the image analysis.

2.7 Flow Cytometry

Flow cytometry was used to assess the cell size and granularity in our experiment. Cells grown and treated in 4 ml DMEM/High glucose medium (HyClone) on 6-well plates were used. First the media (4 ml) was collected in the 15 ml centrifuge tube. Well was washed with 1 ml of PBS and it was also added in the same tube. Cells were then detached from the surface using 1 ml of trypsin for 3-5 minutes. Detached cells were also then added to the same tube. This was performed for all the samples and the final volume was made up to 6 ml in all the cases. After mixing, 200 µL of the solution was added in triplicates in 96 well plates. Forward scatter (FSC) and side scatter (SSC) values were calculated in the BD LSR II Flow cytometer by Dr. Chang-uk Lim.

CHAPTER 3

RESULTS

3.1 Dependence of INoB formation on p21 overexpression

Previous studies performed in our laboratory have shown that INoBs formation can be induced by the induction of p21 in HT1080 p21-9 fibrosarcoma cells (Figure 1.7). HT1080 p21-9 cell line developed in our laboratory has an IPTG inducible p21 (Figure 1.9). To examine the relationship between p21 expression and INoB formation, p21 was differentially induced by using different concentrations of IPTG for different time periods. After 24 hours of treatment with 2.5 µM, 5 µM and 50 µM of IPTG we saw a corresponding increase in the frequency in the number of cells with INoBs with increasing concentration (Figure 3.1 (a)). A similar observation was made following 48 hours treatment of IPTG (Figure 3.1(b)). Those cells in which IPTG (p21 induction) was removed at 24 hours and were allowed to proliferate for another 24 hours didn't show a significant increase in the INoB formation with concentration (Figure 3.1(c)). This result demonstrates that INoB formation is directly related to the level of p21 induction in HT1080 p21-9 cells and a continuous induction of p21 is necessary for the formation of INoBs.

3.2 Effect of Senexin A on p16 and p27 overexpression induced INoBs

To find out the effect of other CDK inhibitors p16 and p27 on the formation of INoBs the respective proteins were induced with 50 µM IPTG in HT1080 p16-5 and HT1080 p27-2 fibrosarcoma cells. Also, the effect of CDK8 inhibitor Senexin A on the formation of INoBs in these cell lines was observed. Previous experiments performed by Dr. Gary P. Schools have shown that formation of INoBs is observed in the HT1080 p16-5 cells treated with 50 µM IPTG for 48 hours (Figure 3.2(a)). p16 was observed to be expressed after IPTG treatment but it did not frequently localize in the INoBs. When INoB formation was analyzed in the HT1080 p16-5 cells treated with 50 µM IPTG for 48 hours with or without 5 µM Senexin A, a strong induction of INoBs in almost 60% of the cell population was observed which was significantly decreased by CDK8 inhibition by Senexin A (Figure 3.2(b)). Induction of p27 by 50 µM IPTG for 48 hours has also been shown to induce the formation of INoBs in HT1080 p27-2 cells (Figure 3.3(a)). Using a similar experimental setup to that used for HT1080 p16-5 cells, the HT1080 p27-2 cell line showed the formation of INoBs in almost 35% of the cells which was not significantly decreased by the inhibition of CDK8 by Senexin A (Figure 3.3(b)).

3.3 INoB formation due to DNA damage

After determining that p21 induction can cause the formation of INoBs we were interested if similar results could be obtained by treating the cells with the DNA damaging agent doxorubicin. To address if DNA damage could cause the formation of INoBs, we treated HCT116 colorectal cancer cells with 20 nM, 40

nM, 80 nM, 160 nM and 320n M concentrations of doxorubicin for 8 h, 24 h, 48 h, 72 h and 96 h. An average of 112 cells in 36 different conditions was scored for the presence of INoBs (Figure 3.4(a)). A general increase in the frequency of cells with INoBs was observed in a time and concentration dependent manner. However, a decrease in the cells with INoBs after the 72 hours time point was observed which may be due to an overall decrease in the cell population by the cytotoxic effect of doxorubicin. We decided to use 160 nM doxorubicin treatment for 48 hours as a standard dosage condition for the future experiments (Figure 3.4(b)). This treatment was able to induce INoB formation in around 55% of the cells without causing a drastic decrease in the cell population.

3.4 Effect of Senexin A on DNA damage induced INoBs in fibrosarcoma cells

Previous experiments have established that INoBs formation induced by p21 and p16 induction can be reduced significantly by CDK8 inhibition by Senexin A in HT1080 fibrosarcoma cells (Figure 1.7 and Figure 3.2(b)). To find out if we can inhibit the DNA damage induced INoBs by CDK8 inhibition, HT1080 p21-9 cells were treated with 30 nM doxorubicin for 48 hours with and without 5 µM Senexin A. Almost 40% of cells with INoBs were observed after this treatment but CDK8 inhibition was insufficient to significantly decrease this formation of INoBs (Figure 3.5(a)). We concluded that 30 nM doxorubicin for 48 hours is not enough to induce a substantial INoB formation in this cell line. The lack of inhibition of INoB formation by Senexin A may be due to an inefficient doxorubicin dose. To determine if a higher dose or longer treatment period could result in INoBs formation which could be inhibited by Senexin A we used 60 nM

of doxorubicin for 48 hours and 30 nM of doxorubicin for 3.5 days as treatment with the same experimental setup. Although we obtained a higher INoB formation (around 50%) in case of 60 nM doxorubicin treatment for 48 hours, Senexin A was not able to decrease the frequency of cells with INoBs (Figure 3.5(b)). In the case of 30 nM doxorubicin treatment for 3.5 days, we observed similar formation of INoBs as 30 nM doxorubicin for 48 hours and no significant effect of CDK8 inhibition by Senexin A was seen (Figure 3.5(c)).

3.5 Involvement of p21 and CDK8 in DNA damage induced INoBs

DNA damage was effective in inducing the formation of INoBs in HCT116 cells (Figure 3.4). To study the involvement of p21 and CDK8 in INoB formation caused by DNA damage we used p21 knockout cells and the CDK8 specific inhibitor Senexin A. Firstly, we treated HCT116 cells with 160 nM of doxorubicin for 48 hours with or without 5 µM Senexin A and then scored the cells for the presence of INoBs. An expected strong induction of INoBs was observed which was significantly decreased by CDK8 inhibition (Senexin A) (Figure 3.6(a)). Secondly, we observed the INoB formation in HCT116 p21 knockout cells after 48 hours treatment with 160 nM doxorubicin as compared to wild type HCT116 cells. The formation of INoBs was significantly lower in p21 knockout cells as compared to the wild type HCT116 cells (Figure 3.6(b)). This suggests that DNA damage-induced expression of p21 and subsequent interaction with CDK8 may be related to the process of formation of INoBs in these cells.

3.6 CDK8 localization after DNA damage

To further characterize the involvement of CDK8 in the possible function of the INoBs we designed the following experiment. Earlier experiments in our laboratory showed CDK8 was frequently in INoBs as a result of p21 induction (Figure 1.7). We wanted to determine if CDK8 localizes in the INoBs formed in the absence of p21. We have already shown that the frequency of cells with INoBs decreases significantly in the HCT116 p21 -/- cells as compared to the wild type. To address this question, HCT116 wt and HCT116 p21 -/- cells were treated with 160 nM doxorubicin for 48 hours and then immunostained for CDK8 to see the localization pattern of CDK8 in both cases. We observed a clear difference in the localization of CDK8 in INoBs. CDK8 was present in the INoBs in 7 of the 8 HCT116 wt cells observed and in 0 of the 8 HCT116 p21 -/- cells (examples are shown in Figure 3.7). It indicates that in the absence of p21 INoBs can form, but the transit of CDK8 to them may be directly or indirectly dependent on p21.

3.7 Quiescence and INoB formation

We now know that we can induce the formation of INoBs by the induction of p21 in HT1080 p21-9 cells (Figure 1.7 and Figure 3.1) and also by DNA damage in HCT116 and HT1080 p21-9, p16-5 and p27-2 cells (Figure 3.2-3.5). The induction of p21 also causes the senescent morphology which is a consequence of the irreversible growth arrest in accelerated senescence. To understand whether we can achieve the formation of INoBs in another type of growth arrest, namely, quiescence (reversible growth arrest) we designed the

following experiment. The serum starvation assay can be used to study quiescence [53]. The cells become growth arrested due to the lack of nutrients in the growth medium which can be reversed by the addition of a fresh growth medium containing the nutrients in the form of fetal calf serum (FCII). HT1080 p21-9 cells were grown with 0.1% and 0.5% of FC II in the DMEM/High glucose growth medium for 48 hours and then the cells were scored for the presence of INoBs. Although cells seems to be bigger in size, in each of the serum starved conditions there was no significant formation of INoBs noticed (Figure 3.8(a)). Among the over 200 cells scored INoBs were observed in less than 3% of the cells in each condition (Figure 3.8(b)). This indicates that while INoBs form as a result of senescence they do not form in induced quiescence.

3.8 Western blot analysis of nucleolar proteins

To understand the dynamics of the nucleolus during the formation of INoBs, we wanted to see what happens to the nucleolar protein levels of p21 and CDK8 when p21 is induced in HT1080 p21-9 cells. Also since we observed that quiescence did not induce INoBs, senescence may be related to the formation of INoBs. Senescent cells, in contrast to the quiescent cells, continue to increase in size, which suggests that continued protein synthesis and continued ribogenesis should be occurring in senescence. Therefore nucleolar RNA polymerase I levels will give us information about the amount of ribogenesis during conditions known to induce INoBs. In Dr. Dmitri Pestov's laboratory, HT1080 p21-9 cells were treated with 0 or 50 µM IPTG for 32 h and then nucleolar extracts were prepared from those cells. These extracts were reconstituted with the nucleolar extract

buffer and then were used for the western blot probing of our desired proteins. Usually anti-β-actin is used to evaluate equal protein loading on the western blot experiments. But in our experiment we were using nucleolar extracts, which should contain no β-actin so we used the nucleolus specific protein, fibrillarin as our loading control. Fibrillarin is the standard nucleolar marker and can be seen to be confined in the nucleolus in both doxorubicin treated and untreated HT1080 p21-9 cells (Figure 3.9(b)). We have observed INoB formation after either p21 induction by IPTG or DNA damage by doxorubicin, hence this can be assumed to be a valid argument that fibrillarin is a marker of nucleolar proteins in our present system of the INoB formation in HT1080 p21-9 cells. We also observed an increase in the cell and nucleolar size due to the induction of p21 within 24 hours which results in a senescent morphology. Because of these size increases, the amount of fibrillarin per mass of protein extract is expected to be lower in the nucleolar extract of IPTG treated cells in comparison to untreated cells (Figure 3.9(a)).10 µg of each extract was loaded in each well. The sample from IPTG-treated cells showed that p21 induction increased the nucleolar accumulation of CDK8 and RNA Polymerase I, with a minor increase in RNA Polymerase II, when normalized to fibrillarin (Figure 3.10(a,b)). This supports our previous immunofluorescence observation of accumulation of CDK8 in the INoBs following p21 induction. Also, the levels of RNA polymerase I are increased which supports our hypothesis that ribogenesis continues in the p21-induced and DNA damaged cells and the resulting protein synthesis is responsible for an increase in the cell size. Perhaps INoBs are in some way involved in ribogenesis during

senescence. In this experiment, we also tried to probe the same blots for p21 but couldn't obtain any signal. The possible reasons for not detecting p21 may be the loading of low amount of the nucleolar extract (10µg) or the deterioration in the quantity of protein in the membrane itself after prolonged storage.

3.9 INoBs and Pol I aggregates

Since we observed that RNA polymerase I levels increase when p21 is induced in the HT1080 p21-9 cells, we wanted to see if INoBs are the site of increased RNA polymerase I localization. To accomplish this we performed the immunocytochemistry for RNA polymerase I after p21 expression. HT1080 p21-9 cells were treated with 0 or 50 µM IPTG and then after 24 hours the CDK8 inhibitor Senexin A (5 µM) was added to some of the coverslips of cells. Senexin A (5 µM) was added 24 hours after IPTG as we wanted to get the maximum induction of p21 which occurs at 24 hours and then see downstream effect of CDK8 inhibition in the formation of INoBs and Pol I aggregates [53]. Cells were fixed and immunofluorescently labeled for RNA polymerase I. In the untreated cells, RNA polymerase I seemed to be localized evenly in the nucleolus (Figure 3.11(a)). We observed the localization of the RNA polymerase I in the form of aggregates usually forming around the periphery and they are completely separate from INoBs after p21 induction by IPTG (Figure 3.11(b)). Hence, we decided to call this peculiar staining of RNA polymerase I as 'Pol I aggregates'. The same slides, in addition to +/- Senexin A were blindly scored for the presence of INoBs and RNA polymerase I aggregates. On an average, 100 cells per condition were scored. We observed that both INoBs and Pol I aggregates

decrease significantly upon CDK8 is inhibited by Senexin A (Figure 3.12(a)). Among the cells counted almost 50% of the cells had both INoBs and Pol I aggregates and cells with only Pol I aggregates were rarely seen (Figure 3.12(b)). Based on these results it can be speculated that INoBs may be needed for the formation of Pol I aggregates.

3.10 INoBs and senescence

We have observed that formation of INoBs is not a characteristic of quiescent cells. We see the formation of INoBs in the p21 induced and DNA damaged HT1080 p21-9 and HCT116 cells which exhibit a senescent morphology. To understand if there is any relation between the INoBs and senescence, we designed the following experiment. Senescent cells are irreversibly growth arrested and have some morphological features which can be assessed by microscopy: increased size, flattened shape and higher degree of granularity. Also the senescent cells express senescence-associated-β-galactosidase enzymatic activity (SA-β-Gal), which can catalyze the digestion of β-galactosides at pH of 6. We used an assay based on production of a blue colored precipitate that results from the cleavage of the β-galactosidase substrate X-Gal. HT1080 p21-9 cells were treated with 50 µM IPTG for 72 hours to induce p21 and 5 µM Senexin A was added 24 hours after the addition of IPTG to see the effect of CDK8 inhibition on the formation of INoBs and more importantly senescence. We observed that INoBs are formed by p21 induction and then the cells having INoBs decreased significantly by CDK8 inhibition (Figure 3.13(a)). On the contrary, senescence measured with SA-β-Gal activity

was unaffected by Senexin A (Figure 3.13(a)). Also we observed that there were not many senescent cells with INoBs and many non-senescent cells can be seen without any INoBs (Figure 3.13(b)). This suggests that may be INoBs formation and SA-β-Gal activity are not related phenomena.

3.11 CDK8 inhibition affects senescent morphology

The two characteristic morphological changes seen in senescent cells are the increase in the cell size and granularity. We observed that CDK8 inhibition by Senexin A was not able to abolish the senescence- associated β-galactosidase activity. We wanted to explore the other aspects of the senescence phenotype affected by Senexin A. We treated HT1080 p21-9 cells with 50 µM IPTG, to induce p21 and hence senescence, and with 0, 1 µM and 5 µM Senexin A for 72 hours. We measured the difference in the size of the cell population as compared to the IPTG untreated cells to observe any significant decrease due to CDK8 inhibition in the senescent cells. Flow cytometry analysis was used to measure the cell size (the forward scatter parameter). We observed that the senescent cell size decreased 3-fold when CDK8 was inhibited by Senexin A in IPTG treated cells (Figure 3.14). In a similar fashion, we looked at the effect of Senexin A on the overall granularity of the cells treated with IPTG (the side scatter parameter in flow cytometric analysis). We did observe some decrease in the granularity of the cells which were treated with IPTG although the decrease was rather weak, especially as compared to the drastic effect on the cell size (Figure 3.15).

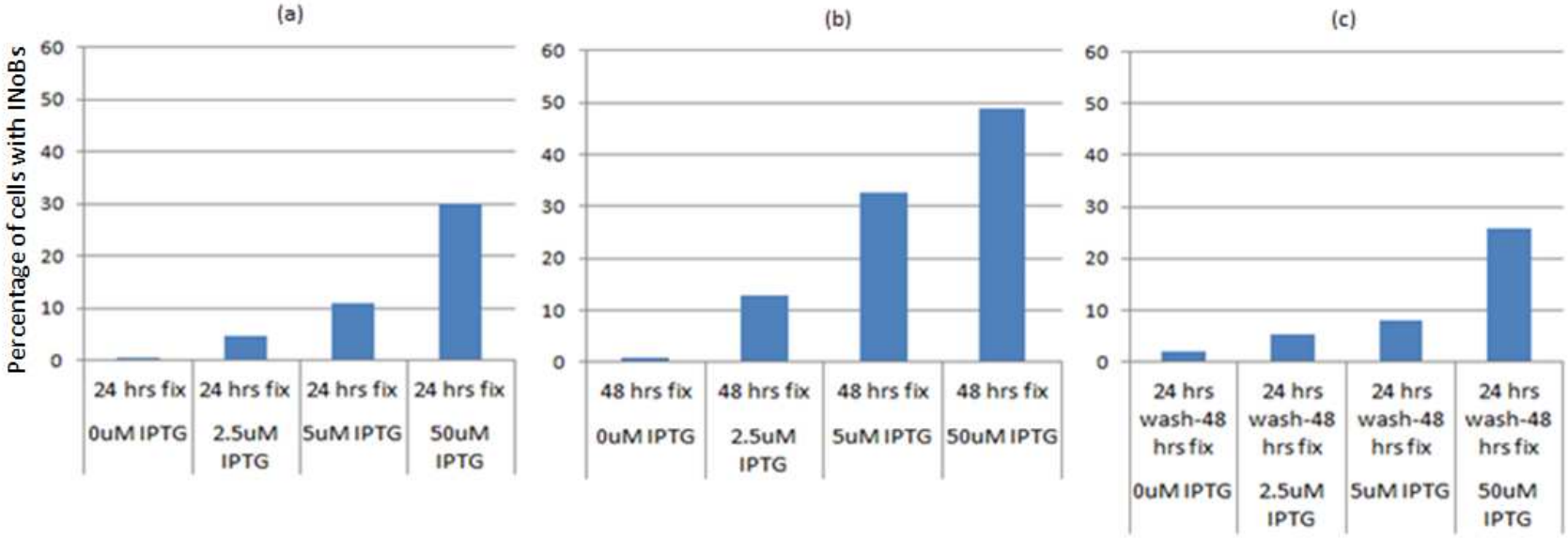

Figure 3.1 Dose dependence of INoB formation on p21 overexpression (a) HT1080 p21-9 cells were treated with 2.5 µM, 5 µM and 50 µM IPTG and the number of cells with or without INoBs were blindly scored on the microscope after 24 hours. (b) Similar treatment and scoring of INoBs was performed in HT1080 p21-9 cells after 48 hours. (c) Medium with IPTG was removed (washed) after 24 hours and fresh medium was added in HT1080 p21-9 cells. INoB scoring was performed after 24 hours of IPTG removal. On an average, 200 cells were scored for the presence of INoBs in each condition for all the experiments using the Differential Interference Contrast (DIC) optics on an Olympus IX81 fluorescent microscope (See methods).

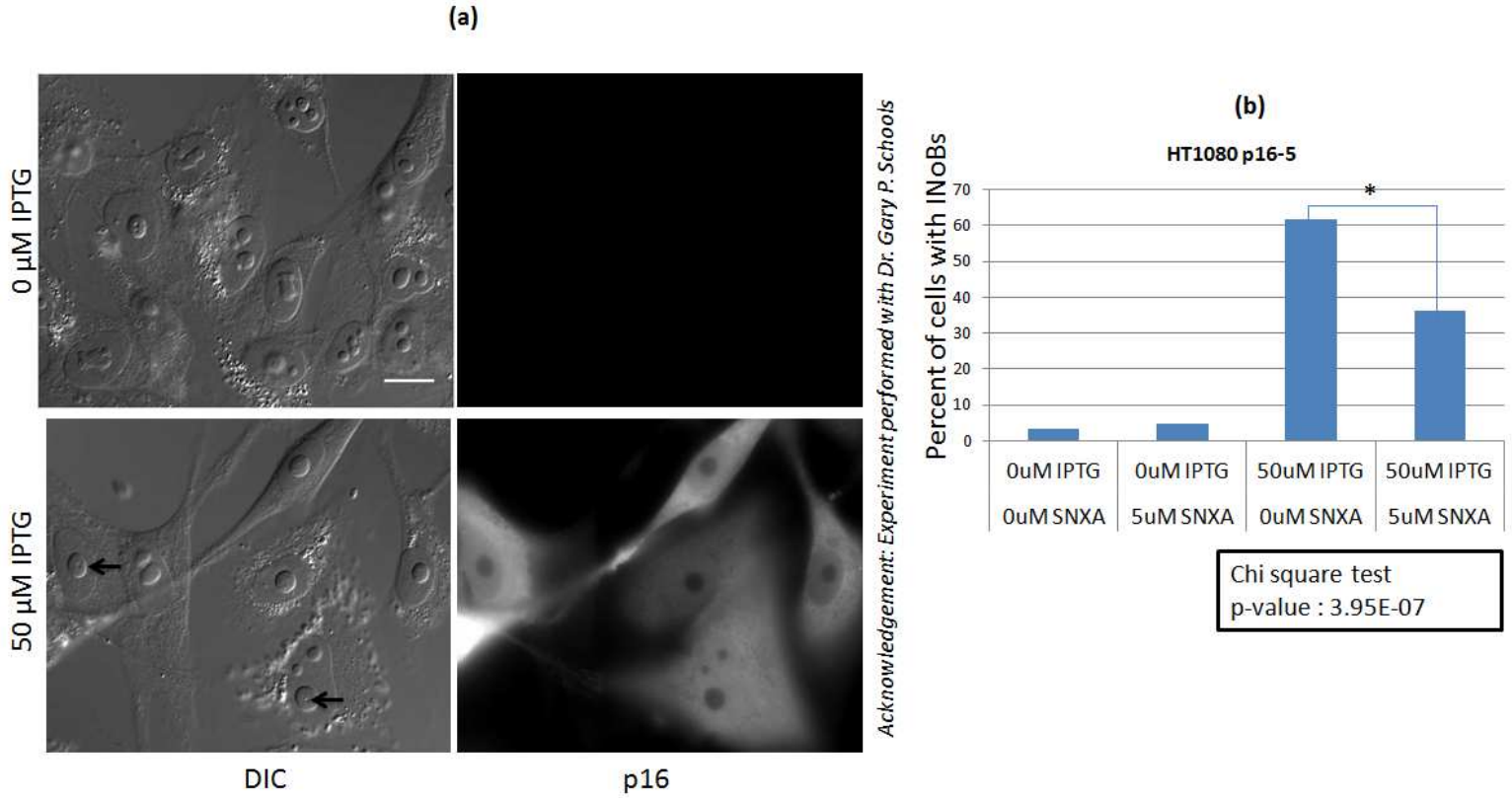

Figure 3.2 Effect of Senexin A on p16 overexpression induced INoBs (a) HT1080 p16-5 fibrosarcoma cells were treated with 50 µM IPTG for 48 hours. INoBs can be observed in DIC images (left panel) while localization of p16 can be seen in the immunostained cells (right panel). Black arrows indicate the cells with visible INoB in the nucleolus. Bar, 8 µm (b) HT1080 p16-5 cells were treated with 50 µM IPTG for 48 hours with and without 5 µM Senexin A. On an average, 200 cells were scored for the presence of INoBs for each condition. A chi-square test was used to measure the statistical significance of difference between the indicated conditions. p-value<0.5 (*)

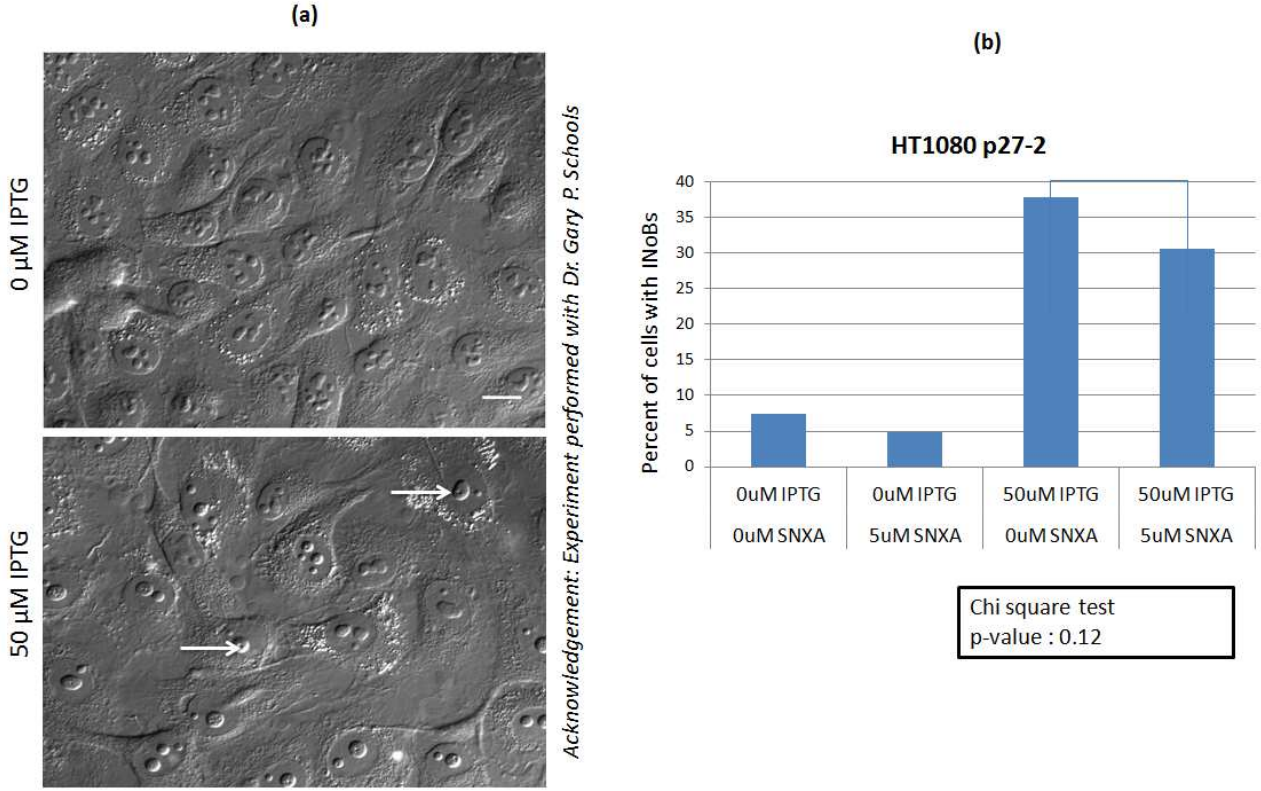

Figure 3.3 Effect of Senexin A on p27 overexpression induced INoBs (a) HT1080 p27-2 cells were treated with 50 µM IPTG for 48 hours shows the formation INoBs in the DIC images. Black arrows indicate the cells with INoBs. Bar, 8 µm (b) HT1080 p27-2 cells were treated with 50 µM IPTG for 48 hours with or without 5 µM Senexin A. On an average, 200 cells were scored for the presence of INoBs in each condition. A chi-square test was used to measure the statistical significance of difference between the indicated conditions. p-value<0.5 (*)

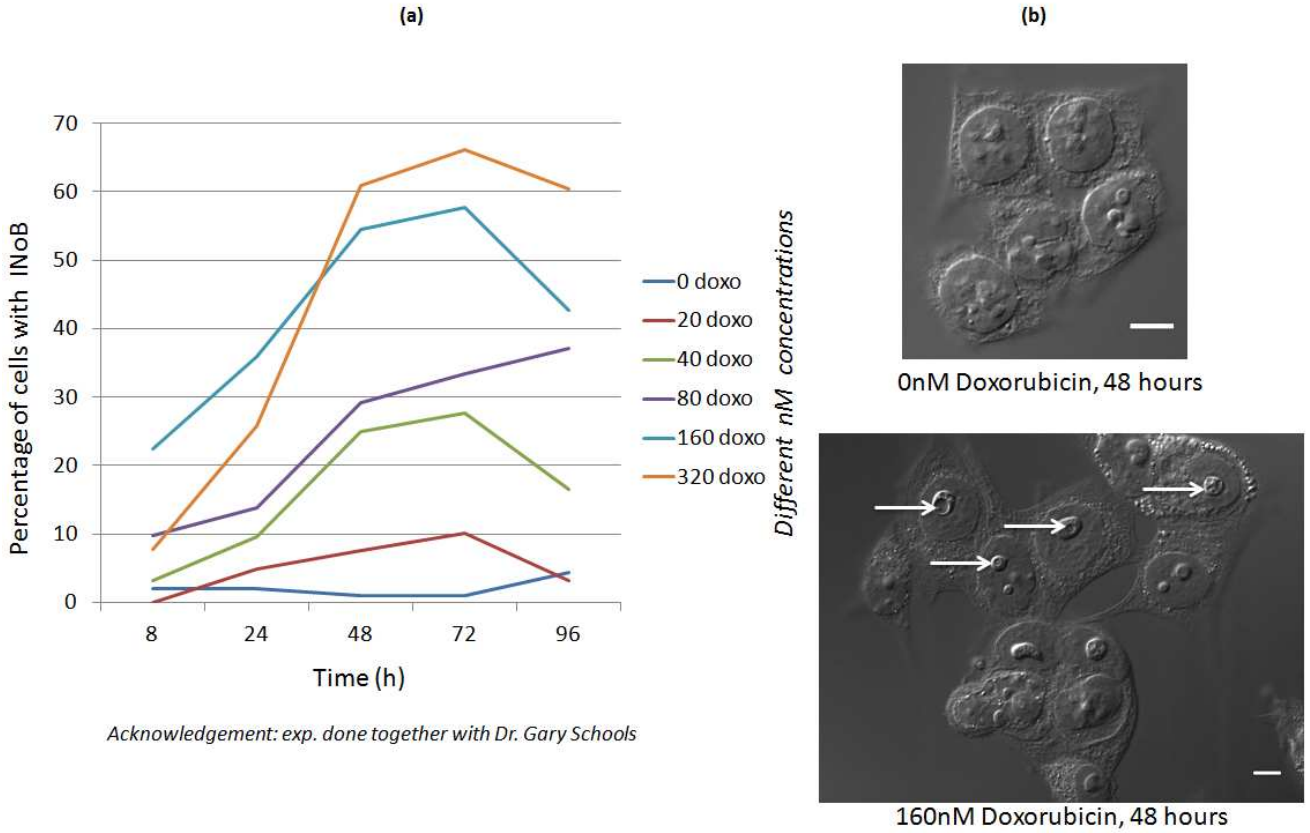

Figure 3.4 INoB formation due to DNA damage (a) HCT116 cells were treated with 0-320 nM doxorubicin for 8-96 h and then the cells were scored for the presence of DIC-visible INoBs. On an average, 112 cells per condition were scored. Greater than 50% of the cells treated with 160 nM and 320 nM doxorubicin had INoBs at 48 and 72 hours.(b) Black arrows indicating the cells with INoBs in HCT116 cells after 160 nM doxorubicin treatment for 48 hours as compared to untreated cells. Bars, 8 µm.

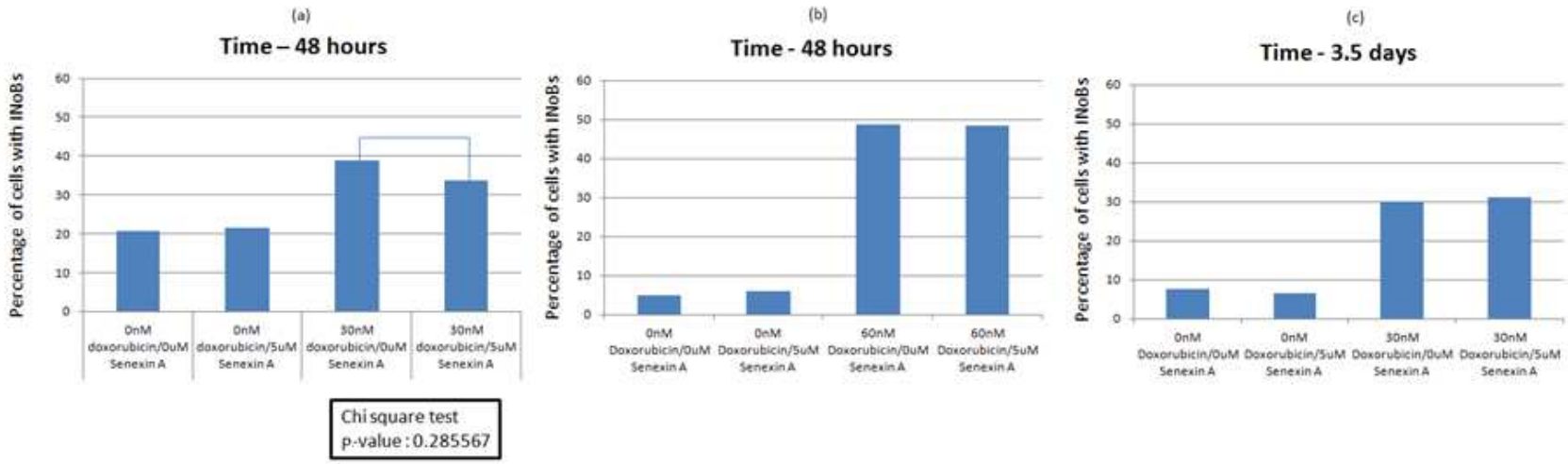

Figure 3.5 Effect of Senexin A on DNA damage induced INoBs in fibrosarcoma cells (a) HT1080 p21-9 cells treated with 30 nM doxorubicin for 48 hours with and without 5 µM senexin A. On an average, 200 cells were scored for each condition. A chi-square test was used to measure the statistical significance of difference between the indicated conditions. p-value<0.5 (*) (b) HT1080 p21-9 cells were treated with 60 nM doxorubicin for 48 hours with and without 5 µM senexin A. On an average, 100 cells were scored for each condition.(c) HT1080 p21-9 cells were treated with 30 nM doxorubicin for 3.5 days with and without 5 µM senexin A. On an average, 100 cells were scored for each condition.

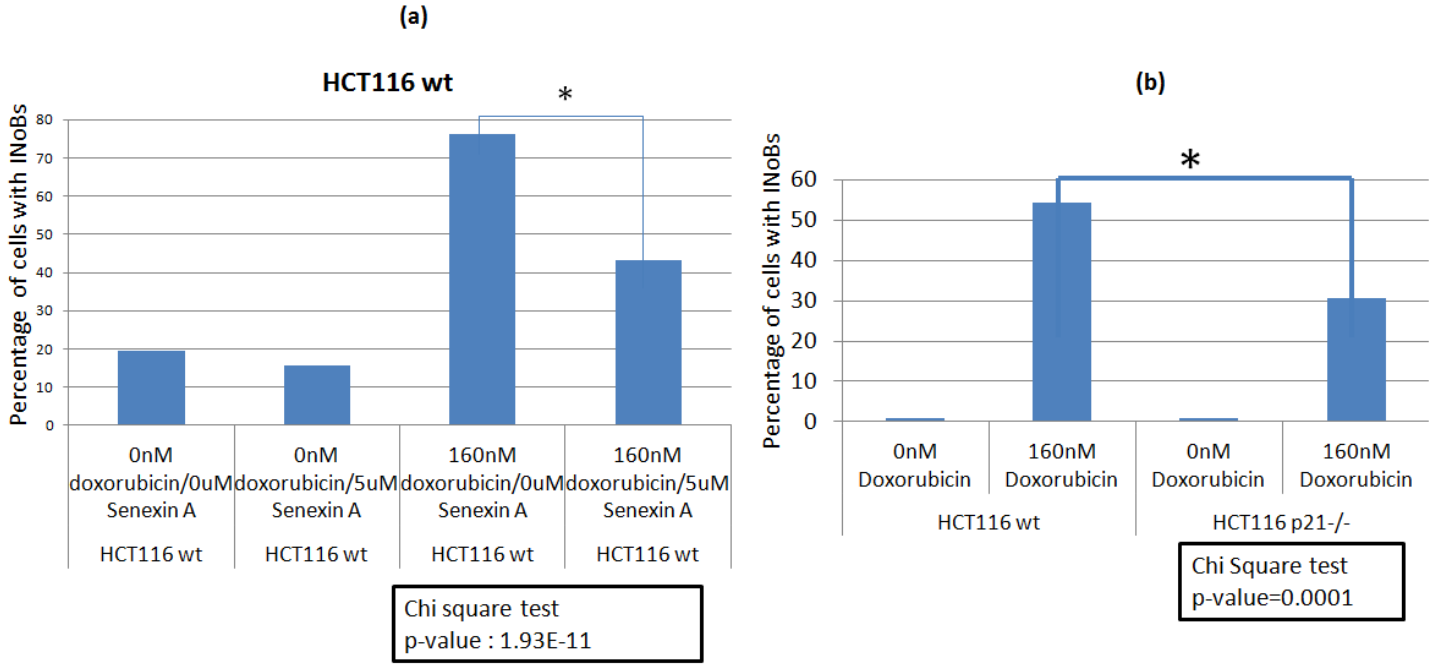

Figure 3.6 Role of p21 and CDK8 in DNA damage induced INoBs (a) HCT116 colorectal cancer cells were treated with 160 nM doxorubicin with or without 5 μM senexin A for 48 hours, and then cells were scored for the presence of INoBs in each condition. On an average, 200 cells were scored in each condition. (b) HCT116 wt and HCT116 p21-/- cells were treated with 160 nM doxorubicin for 48 hours and then scored for the presence of INoBs. On an average, 100 cells were scored for the presence of INoBs in each condition. A chi-square test was used to measure the statistical significance of the difference between the indicated conditions. p-value<0.5 (*)

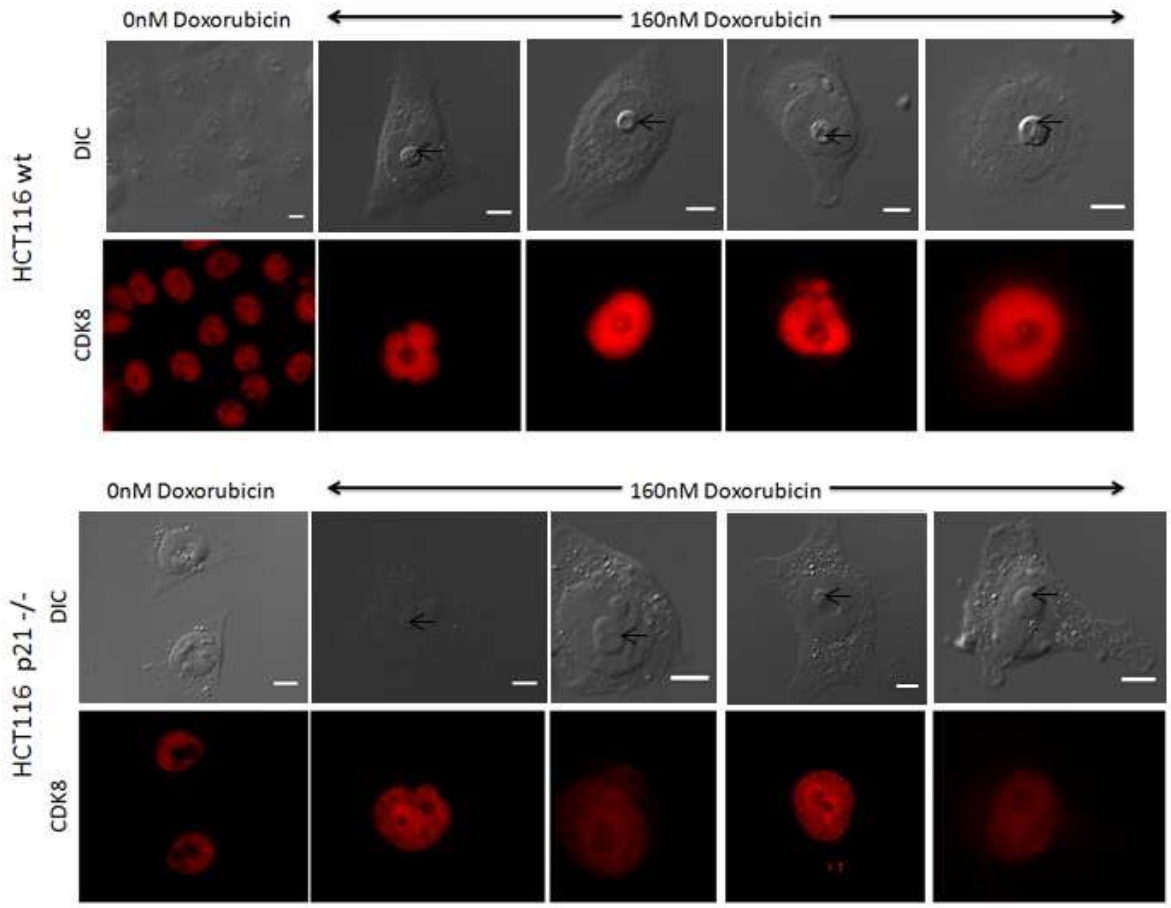

Figure 3.7 CDK8 localization in DNA damage induced INoBs. HCT116 wt and HCT116 p21-/- cells were treated with 160 nM doxorubicin for 48 hours and then immunostained to assess the localization of CDK8. Black arrows show the location of INoBs in the DIC images. Bars, 8 µm.

(a)

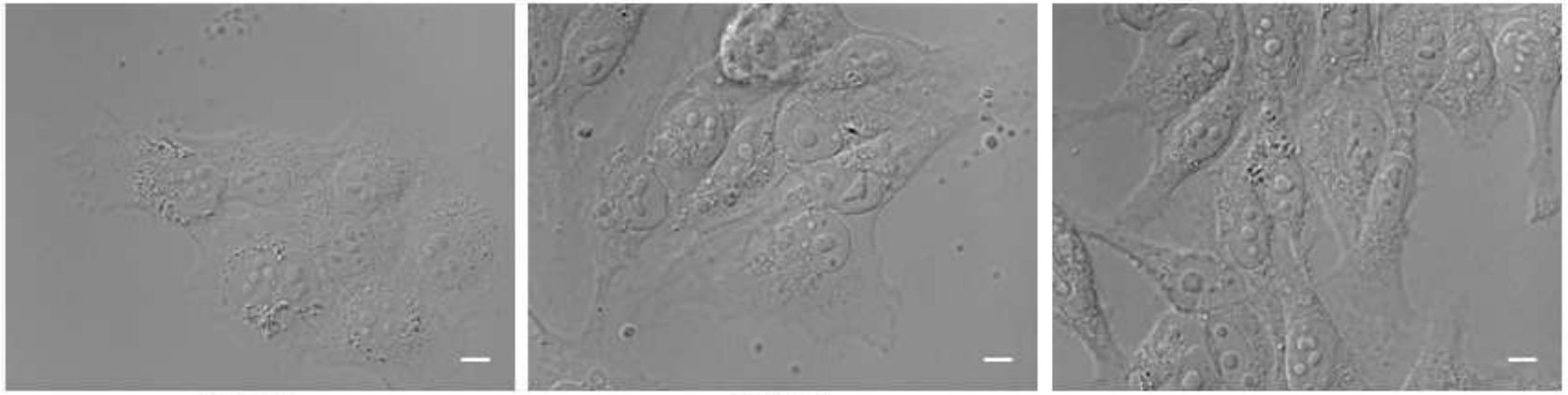

10% FC II

0.1% FC II

0.5% FC II

(b)

FC II percentage	Total cells counted	Cells with INoBs
10%	206	1
0.10%	203	5
0.50%	201	6

Figure 3.8 Quiescence and INoB formation (a) Representative images showing the HT1080 p21-9 cells grown in medium containing normal 10%, 0.1% and 0.5% Fetal Calf Serum (FC II) for 48 hours. Bar, 8 µm (d) Table showing the number of cells with INoBs observed in each condition. On an average, 200 cells in each condition were scored for the presence of INoBs.

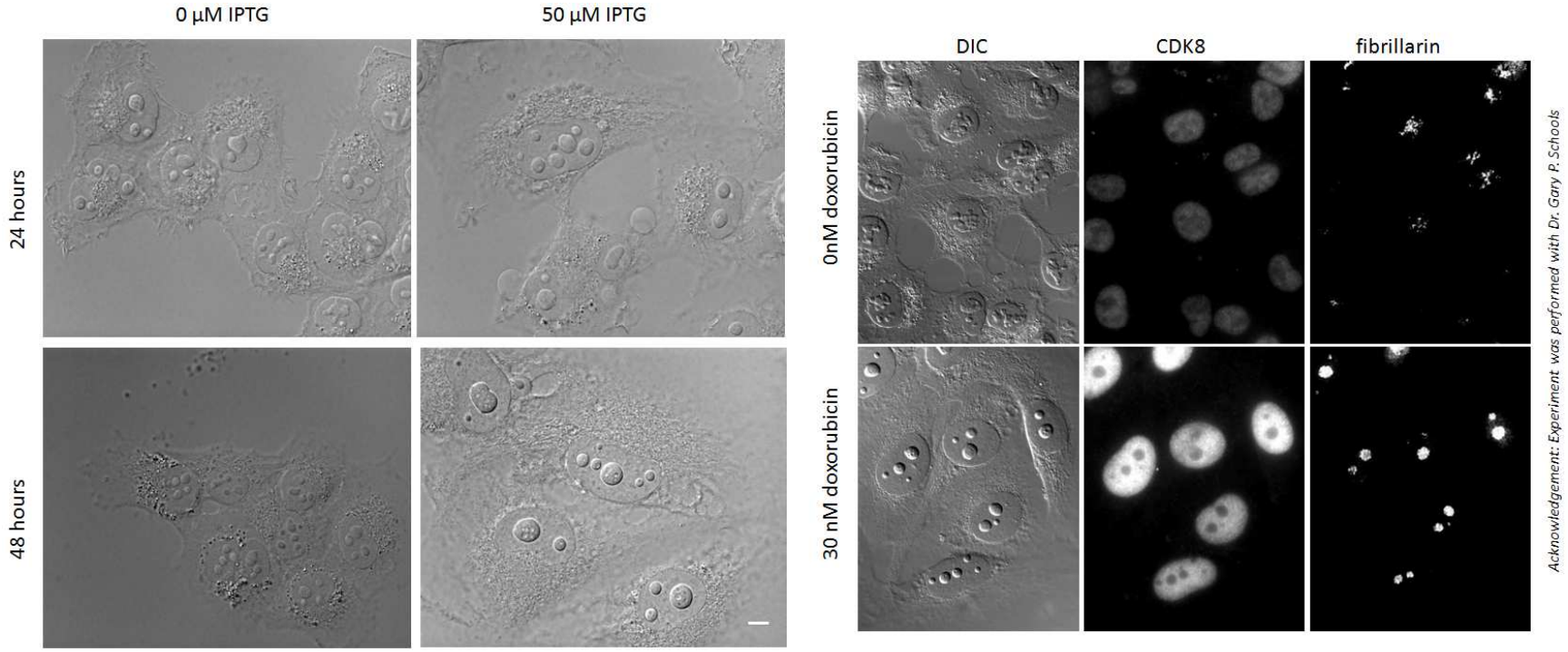

Figure 3.9 p21 induced increase in cell size and fibrillarin as nucleolar marker (a) HT1080 p21-9 cells that were treated with 50 µM IPTG for 24 hours and 48 hours show an increase in the cell and nucleolus size. Bar, 8 µm (b) HT1080 p21-9 cells treated with 30 nM doxorubicin for 48 hours. DIC images show the increase in the cell size. Immunocytochemistry images show the CDK8 localization in the nuclear region and fibrillarin localization in the nucleolus.

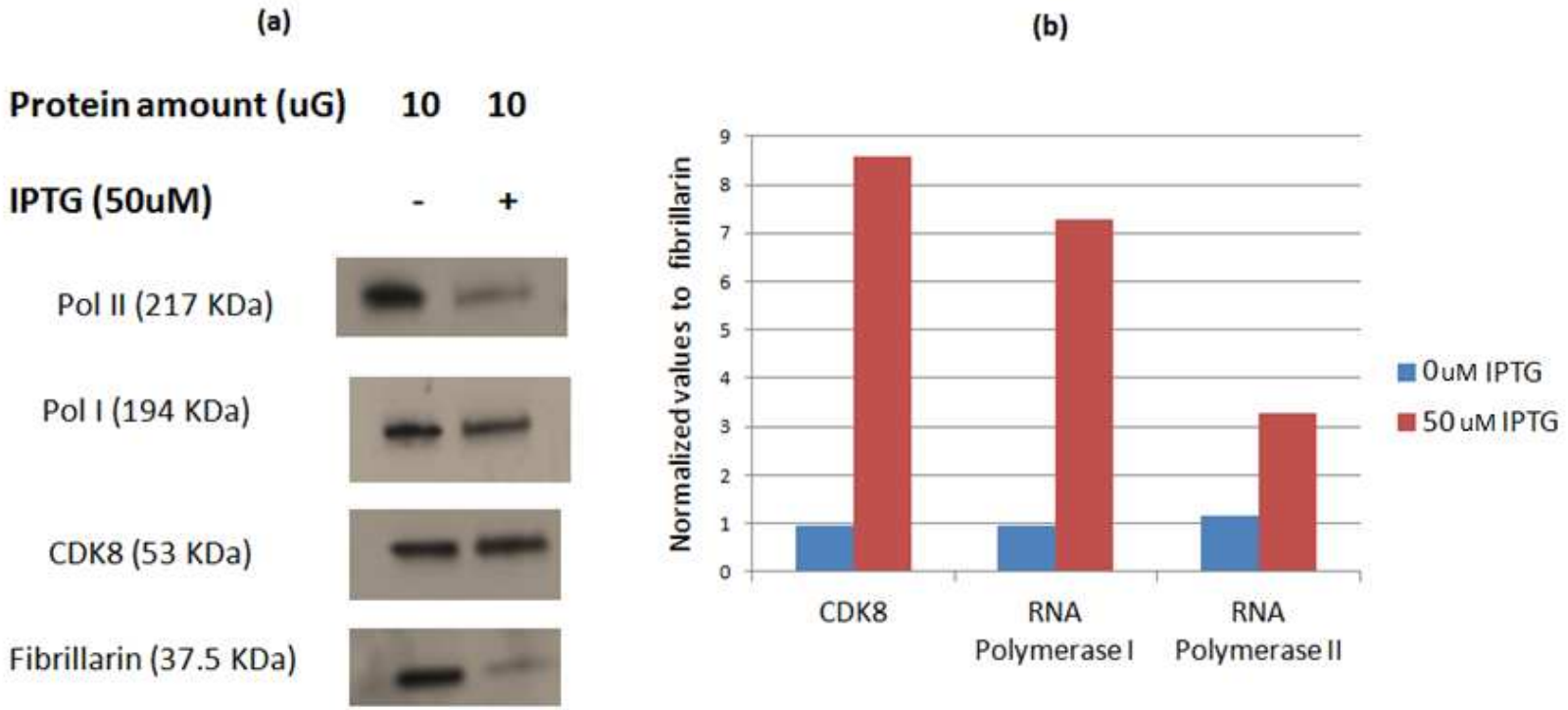

Figure 3.10 Western blot analysis of nucleolar proteins (a) HT1080 p21-9 cells were treated with 0 or 50 µM IPTG and then nucleolar extracts were prepared from those cells in Dr.Dmitri Pestov's laboratory (UMDNJ). A western blot was performed using 10 µg of these extracts in each lane. The same membranes were probed for RNA polymerase II (Mol. Wt.: 217KDa), RNA polymerase I (Mol. Wt.:194KDa), CDK8 (Mol. Wt.:53KDa) and Fibrillarin (Mol. Wt.: 37.5KDa). (b) The quantities of CDK8, RNA polymerase I and RNA polymerase II were normalized to the quantity of fibrillarin in control (0 µM IPTG) and 50 µM IPTG treated samples.

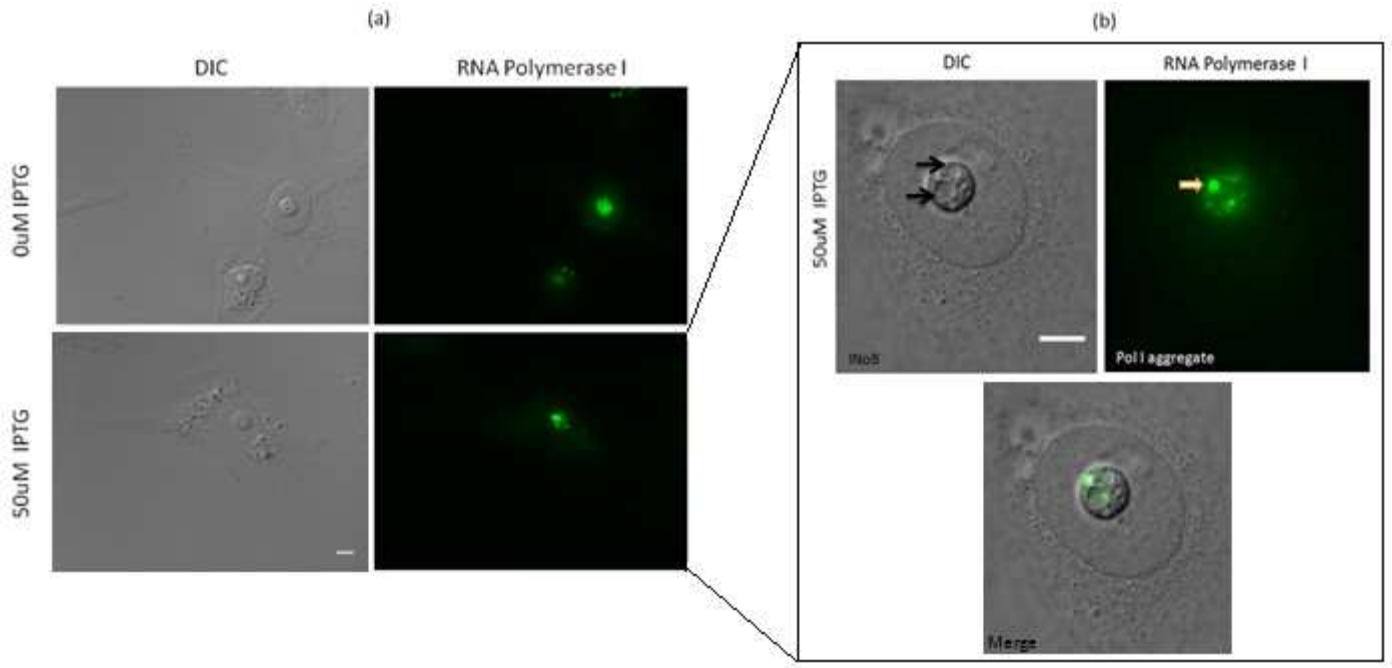

Figure 3.11 INoBs and Pol I aggregates form at distinct regions in the nucleolus (a) HT1080 p21-9 cells were treated with 50 µM IPTG for 72 hours. DIC images show the position of nucleolus for the comparison of RNA Polymerase I localization with and without the induction of p21 by IPTG. Bar, 8 µm (b) RNA polymerase I aggregates are seen as distinctly stained puncta in the nucleolus of cell treated with 50 µM IPTG. INoBs can be clearly seen as separate entities in the merge image of the same cell. Bar, 8 µm.

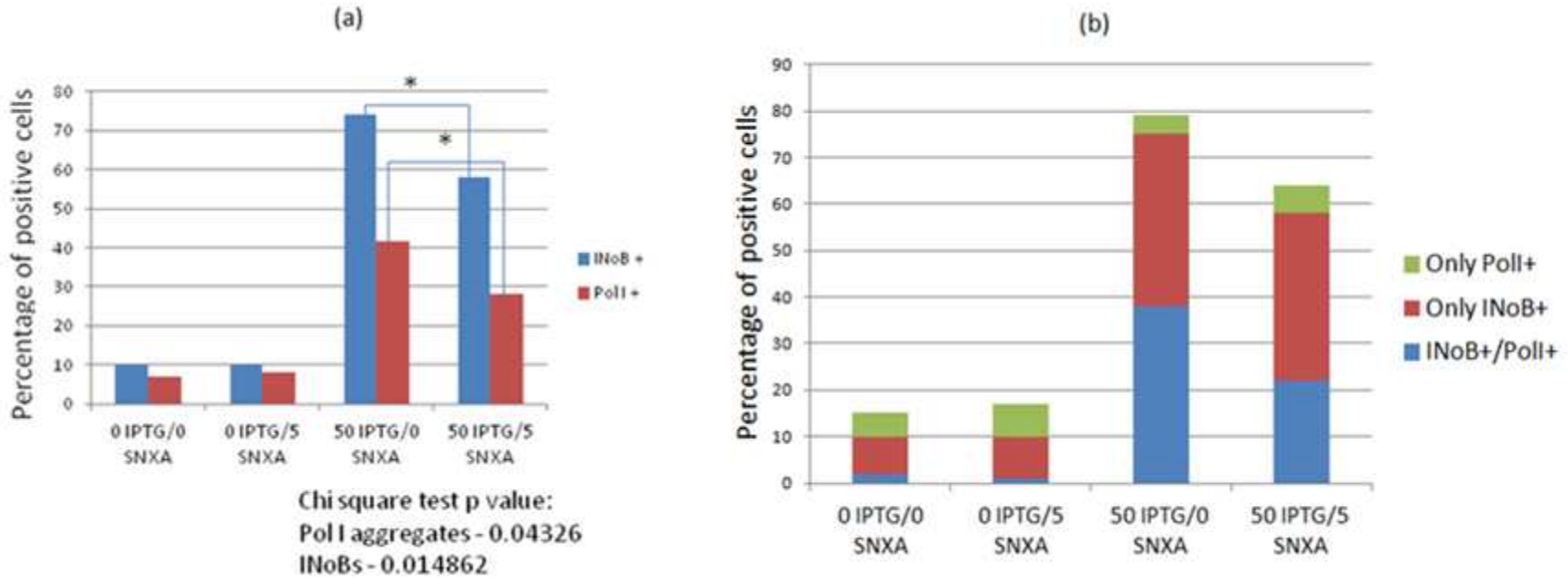

Figure 3.12 Effect of Senexin A on Pol I aggregates formation (a) HT1080 p21-9 cells treated with IPTG for 72 hours with or without Senexin A. Senexin A in this experiment was added 24 hours after the addition of IPTG. Cells were scored for the presence of INoBs and Pol I aggregates (see methods). On an average, 100 cells were scored in each condition. (b) Population distribution of the cells which only have Pol I aggregates (PolI+), only INoBs (INoB+) or both Pol I aggregates and INoBs (INoB+/PolI+) in same experiment as (a). A chi-square test was used to measure the statistical significance, p-value< 0.05 (*)

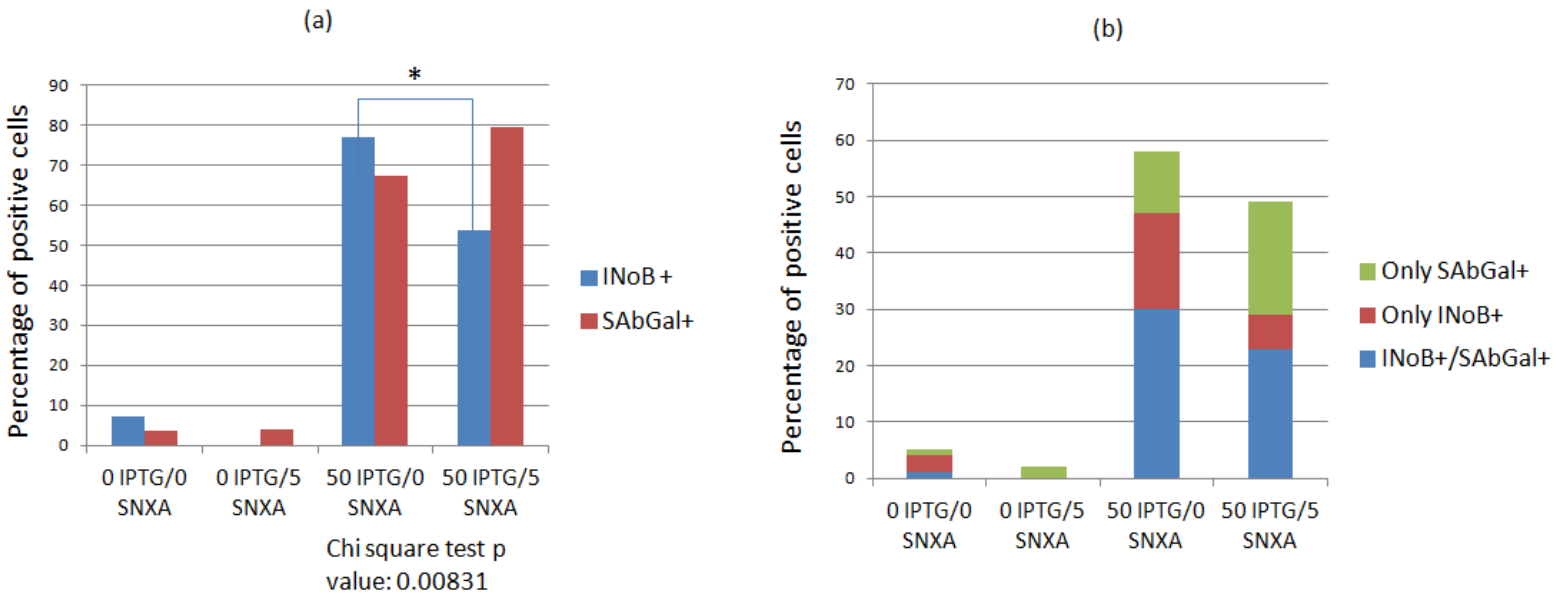

Figure 3.13 INoBs and cell senescence (a) HT1080 p21-9 cells were treated with 50 µM IPTG for 72 hours with or without Senexin A. Senexin A (5 µM) was added after 24 hours of IPTG addition. On an average, 50-60 cells were scored in each condition for the presence of INoBs and the characteristic blue Senescent Associated β-galactosidase (SA β-Gal) staining. A chi-square test was used to measure the statistical significance of change in the indicated conditions. p-value<0.5 (*) (b) Population distribution of the same experiment showing the numbers of cells which were only senescent (SAbGal+), only had INoBs (INoB+) or were both senescent and had at least one INoB (INoB+/SAbGal+).

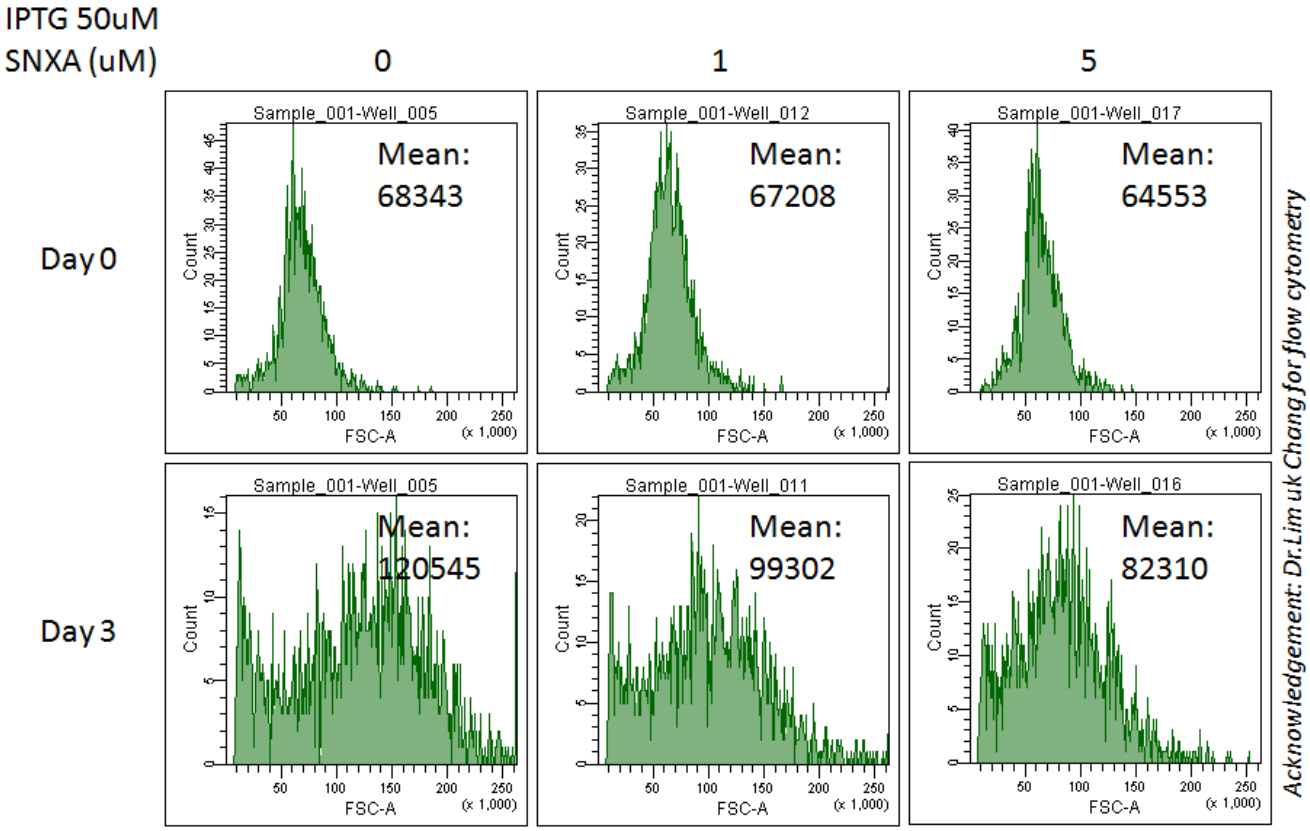

Figure 3.14 CDK8 inhibition affects p21 induced increase in cell size. HT1080 p21-9 cells were treated with 50µM IPTG and 0, 1 or 5 µM Senexin A and the cell size was measured days after the treatment. Flow cytometric analysis of the forward scatter of the cell population was performed which gives the measure of the cell size. Mean scatter values are indicated for each condition in the box.

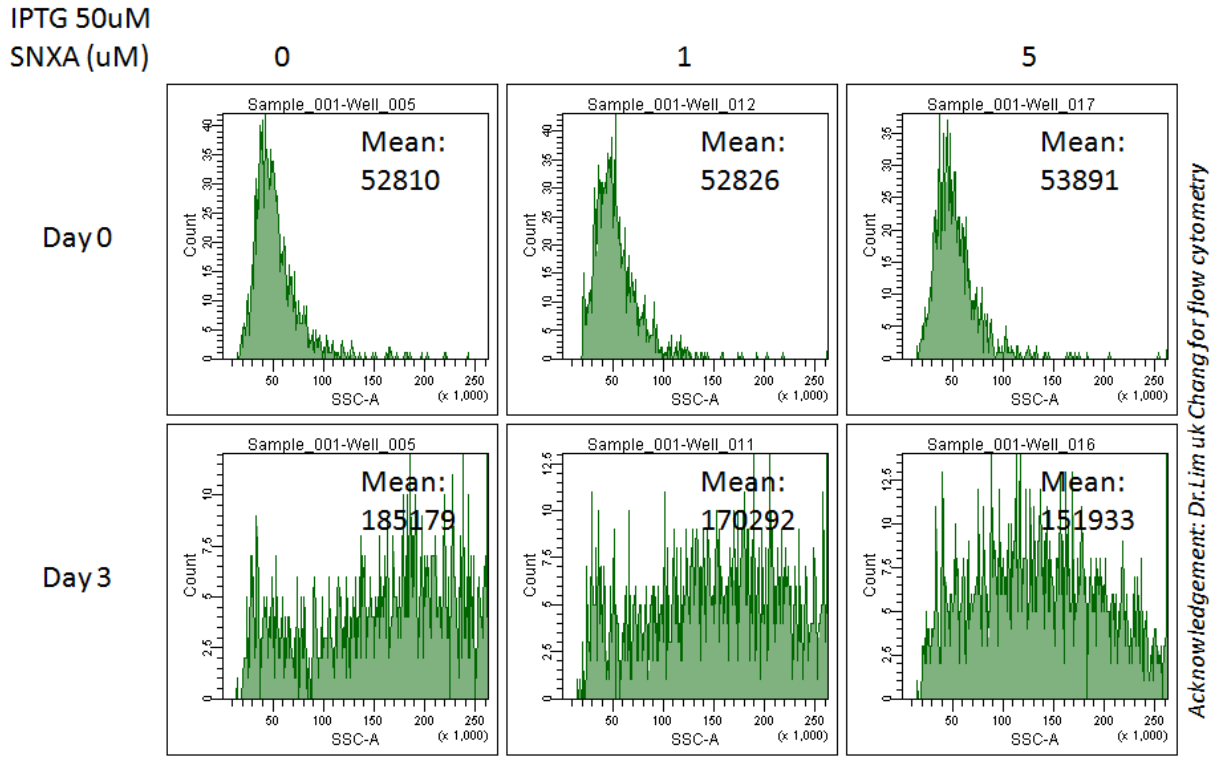

Figure 3.15 CDK8 inhibition affects p21 induced increase in cell size. HT1080 p21-9 cells were treated with 50 µM IPTG and 0, 1 or 5 µM senexin A and the cell granularity was measured 3 days after the treatment. Flow cytometric analysis of the side scatter of the cell population was performed which gives the measure of the cell granularity. Mean scatter values are indicated for each condition in the box.

CHAPTER 4

DISCUSSION

The nucleolus is a dynamic structure primarily involved in the ribogenesis process. Recent studies have indicated its role in other functions of the cell, stress response being one of them. Nucleolar protein content and morphology undergo characteristic changes under the effect of several types of stress [10]. Nucleolar segregation and disruption is the most observed and studied among those morphological changes. Nucleolar segregation is defined by the condensation and separation of the FC and GC, together with the formation of ‘‘nucleolar caps’’ around the nucleolus [15]. On the other hand, nucleolar disruption is characterized by the unraveling of FC [16, 84].

Spherical structures appearing inside the nucleolus after the induction of p21 in HT1080 fibrosarcoma cells were first observed in our laboratory by Dr. Gary P. Schools. Recent findings by a different group [27] showed localization of p21 in similar nucleolar inclusions called Intranucleolar Bodies (INoBs) and our results with the CDK8 inhibitor led us to further explore these novel structures. Some of the initial microscopy experiments established that these INoBs emerge after p21 induction and are positive for p21 and CDK8 which may be involved in INoB formation. Interestingly, the formation of these INoBs was significantly decreased by a small molecule CDK8 inhibitor, Senexin A [29].

The current study was initiated by characterizing the conditions causing the formation of the INoBs and their possible effects on RNA transcription. We used HT1080 fibrosarcoma cell lines with IPTG inducible p21, p16 and p27 to analyze the effect of CKIs on the formation of INoBs. These CKIs effectively caused the formation of INoBs in 35 to 50% of the cells within 48 hours (Figures 3.1-3.3). In case of p21 this effect was also confirmed to be dose dependent. Moreover, CDK8 inhibition by Senexin A caused the reduction in the frequency of cells with INoBs in case of p21 and p16 induction (Figure 1.7 and 3.2). CDK8, which is activated by p21, is involved in many transcriptional programs related to carcinogenesis and the stem-cell phenotype [72, 85] including chemotherapy induced tumor promoting paracrine activities [29]. These results indicate that p21 and CDK8 may be involved in the formation of INoBs and regulation of currently unknown functions of these INoBs.

As both p21 and CDK8 are involved in the DNA damage induced changes in the cell, we proposed to observe the effect of DNA damage on the dynamics of the formation of INoBs. Both the wild type HCT116 colon carcinoma cell line and HCT116 p21-/- cell line where p21 has been completely knocked out were used in these experiments. As expected we saw a strong induction of INoBs in these cell lines after the treatment with DNA damaging drug doxorubicin in more than 50% of the cells which was significantly reduced by CDK8 inhibition in wt HCT116. Interestingly, although we saw an overall significant decrease in the number of cells with DNA damage-induced INoBs in HCT116 p21 -/- cells, there were a significant number of cells having INoBs as compared to the control cells.

This indicated that INoBs may also be induced by mechanisms different than those involving p21. As further characterization of p21-independent INoBs, we observed that the INoBs formed in p21 knockout cells did not have CDK8 in INoBs as the wild type p21 cells did. Therefore, it is possible that there are two kinds of INoBs, one induced by p21 and CDK8 and the other by a different mechanism(s). In future experiments, it will be important to assess the effect of Senexin A on INoB formation and the localization of CDK8 in HCT116 p21-/- cells treated with doxorubicin or other DNA damaging agent. CDK8 may play a role in INoB formation or pol I aggregation even if it is not in these structures.

CDK inhibitors, such as p21, are involved in cell cycle arrest under various stimuli [46]. This growth arrest can be reversible (quiescence), occurring during nutrient stress or irreversible (senescence), happening in response to DNA damage or other factors. Serum starvation-induced quiescence in HT1080 p21-9 cells did not cause INoB formation (Figure 3.8). p21 induction and DNA damage both cause the senescent phenotype. Senescent cells remain metabolically and transcriptionally active. In contrast, quiescent cells should be much less transcriptionally active especially if the quiescence is induced by serum starvation. We argued that INoB formation may be related to the transcription regulation in the nucleolus. Western blot analysis of nucleolar extracts after p21 induction shows a higher amount of CDK8 and RNA polymerase I normalized by nucleolar marker fibrillarin. CDK8 forms a complex with Cyclin C, Med12 and Med13 called CDK module which interacts with the small Mediator complex [86] and affects RNA polymerase II mediated transcription [87] [88]. Also when

HT1080 p21-9 cells were stained for RNA polymerase I after p21 induction, we saw it as condensed in aggregates on the periphery of the nucleolus. Pol I aggregates are localized at completely different parts of the nucleolus than INoBs, and like INoBs, their numbers can be significantly decreased by Senexin A treatment. The population distribution of the cells scored for both INoBs and Pol I aggregates showed that Pol I aggregates are found together with INoBs in most of the cells (Figure 3.12). This indicates that these Pol I aggregates are possibly functionally related to INoBs or that both structures are the consequence of a common change in the nucleolus. To further investigate the association between transcription and INoBs, we can perform Ethylene Uridine (EU) incorporation assays and *In situ* hybridization assays to assess the active transcription sites within the nucleolus under the conditions, which induce formation of INoBs and Pol I aggregates.

The HT1080 p21-9 cells line is a versatile model system to study senescent phenotype since senescence can be brought on by treatment with DNA damaging agents or IPTG. We wanted to determine if there is a correlation between the different aspects of this senescence, SA-β-Gal activity, cell size and granularity, and the formation of INoBs. INoBs and SA-β-Gal positive cells were not found to be correlated (Figure 3.13). Furthermore, Senexin A did not affect the frequency of SA-β-Gal positive cells as compared to the INoBs formation. However, the flow cytometry analysis of the HT1080 p21-9 cells treated with IPTG and Senexin A for 3 days show that CDK8 inhibition greatly reduced the increase in the cell size that occurs with senescence and also had an effect on

granularity which are characteristic features of senescent phenotype. In future experiments, it will be interesting to study the long term effect of Senexin A on the cell size and granularity and its correlation with the presence of INoBs in the cells.

Figure 4.1 summarizes the results of this study as described below. We saw that CDK inhibitors p21, p16 and p27 induction and DNA damage can cause an increase in INoB formation which can be reduced by CDK8 inhibition with Senexin A. Also, p21 induction causes an increase in the formation of Pol I aggregates and senescence associated cell size and granularity which are decreased by CDK8 inhibition with Senexin A. Although p21 induction causes cell senescence it can't be reduced by Senexin A treatment. Pol I aggregates seems to form in the cells with INoBs and hence there is a possibility that INoB's function maybe related to rRNA transcription. In case of HCT116 p21-/- cells, we didn't see CDK8 localization in DNA damage induced INoB formation (Figure 3.7) which indicates they may be different kind of INoBs (Type 2 INoBs) induced by p21-independent mechanism(s). Missing links (denoted by sign '?' in Figure 4.1) in the study show where further studies are needed to understand the relationships between the indicated processes.

Structures similar to INoBs have been observed previously by other groups [27, 28], and this study provides important information regarding their formation and relation to various cellular processes. We observed that either by induction of CDK inhibitors or by DNA damage the nucleolus undergoes structural changes which may have a downstream effect on rRNA transcription,

DNA damage response or senescence. Future research plans can be designed to investigate the relationship between formation of INoBs and rRNA transcription to further define the function of nucleolus as the cellular “fighting ground” against stress. Growth arrest (senescence) provides a possible route on how those changes are being manifested morphologically. Observation of the presence of different type of INoBs after DNA damage provides an alternate approach in studying the overall stress response. Future experiments will be able to successfully connect all these processes through the indicated missing links (indicated by ‘?’) (Figure 4.1) and unfold the biological mechanism taking place in the nucleolus under stress.

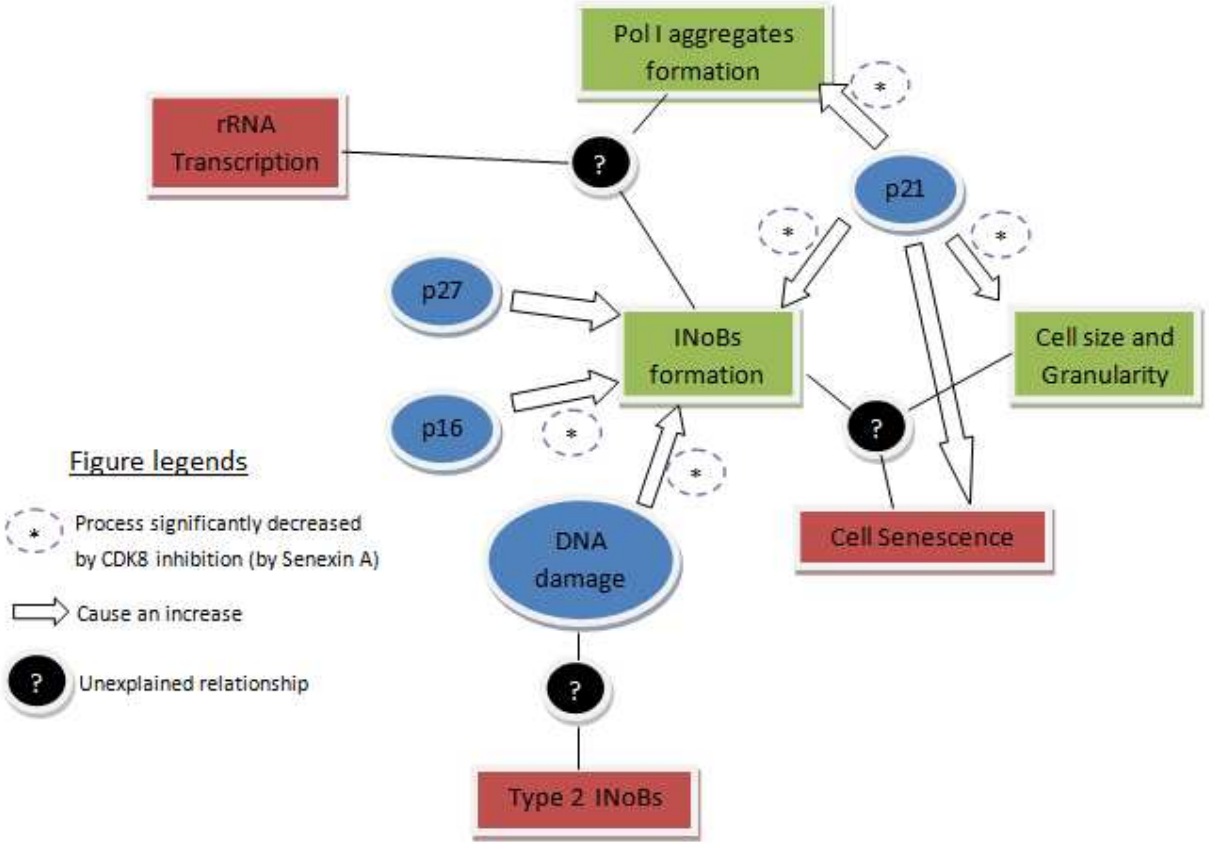

Figure. 4.1 Schematic diagram showing the summary of the study on the effect CDK inhibitors and DNA damage in the restructuring of the nucleolus and its possible relation to DNA damage response, rRNA transcription and cell senescence.

REFERENCES

1. Perry, R.P., *The Cellular Sites of Synthesis of Ribosomal and 4s Rna.* Proc Natl Acad Sci U S A, 1962. **48**(12): p. 2179-86.
2. Ritossa, F.M. and S. Spiegelman, *Localization of DNA Complementary to Ribosomal Rna in the Nucleolus Organizer Region of Drosophila Melanogaster.* Proc Natl Acad Sci U S A, 1965. **53**: p. 737-45.
3. Andersen, J.S., et al., *Nucleolar proteome dynamics.* Nature, 2005. **433**(7021): p. 77-83.
4. Melese, T. and Z. Xue, *The nucleolus: an organelle formed by the act of building a ribosome.* Curr Opin Cell Biol, 1995. **7**(3): p. 319-24.
5. Fatica, A. and D. Tollervey, *Making ribosomes.* Curr Opin Cell Biol, 2002. **14**(3): p. 313-8.
6. Cmarko, D., et al., *Ultrastructural analysis of nucleolar transcription in cells microinjected with 5-bromo-UTP.* Histochemistry and cell biology, 2000. **113**(3): p. 181-187.
7. Casafont, I., et al., *The giant fibrillar center: a nucleolar structure enriched in upstream binding factor (UBF) that appears in transcriptionally more active sensory ganglia neurons.* Journal of structural biology, 2007. **159**(3): p. 451-461.
8. Biggiogera, M., et al., *Simultaneous immunoelectron microscopic visualization of protein B23 and C23 distribution in the HeLa cell nucleolus.* Journal of Histochemistry & Cytochemistry, 1989. **37**(9): p. 1371-1374.
9. Ahmad, Y., et al., *NOPdb: Nucleolar Proteome Database--2008 update.* Nucleic Acids Res, 2009. **37**(Database issue): p. D181-4.
10. Boulon, S., et al., *The nucleolus under stress.* Mol Cell, 2010. **40**(2): p. 216-27.
11. Ong, S.E., et al., *Stable isotope labeling by amino acids in cell culture, SILAC, as a simple and accurate approach to expression proteomics.* Mol Cell Proteomics, 2002. **1**(5): p. 376-86.
12. Boisvert, F.M., et al., *A quantitative proteomics analysis of subcellular proteome localization and changes induced by DNA damage.* Mol Cell Proteomics, 2010. **9**(3): p. 457-70.
13. Cohen, A.A., et al., *Dynamic proteomics of individual cancer cells in response to a drug.* Science, 2008. **322**(5907): p. 1511-6.
14. Al-Baker, E.A., et al., *Analysis of UV-induced damage and repair in young and senescent human dermal fibroblasts using the comet assay.* Mech Ageing Dev, 2005. **126**(6-7): p. 664-72.

15. Shav-Tal, Y., et al., *Dynamic sorting of nuclear components into distinct nucleolar caps during transcriptional inhibition.* Mol Biol Cell, 2005. **16**(5): p. 2395-413.
16. David-Pfeuty, T., *Potent inhibitors of cyclin-dependent kinase 2 induce nuclear accumulation of wild-type p53 and nucleolar fragmentation in human untransformed and tumor-derived cells.* Oncogene, 1999. **18**(52): p. 7409-22.
17. Rubbi, C.P. and J. Milner, *Disruption of the nucleolus mediates stabilization of p53 in response to DNA damage and other stresses.* EMBO J, 2003. **22**(22): p. 6068-77.
18. Kruhlak, M., et al., *The ATM repair pathway inhibits RNA polymerase I transcription in response to chromosome breaks.* Nature, 2007. **447**(7145): p. 730-4.
19. Carmo-Fonseca, M., J. Ferreira, and A.I. Lamond, *Assembly of snRNP-containing coiled bodies is regulated in interphase and mitosis--evidence that the coiled body is a kinetic nuclear structure.* J Cell Biol, 1993. **120**(4): p. 841-52.
20. Handwerger, K.E., et al., *Heat shock induces mini-Cajal bodies in the Xenopus germinal vesicle.* J Cell Sci, 2002. **115**(Pt 10): p. 2011-20.
21. Mekhail, K., Rivero-Lopez, L., Khacho, M., and Lee, S.. *Restriction of rRNA synthesis by VHL maintains energy equilibrium under hypoxia*. Cell Cycle, 2006 (5): p. 2401–2413
22. Burger, K., et al., *Chemotherapeutic drugs inhibit ribosome biogenesis at various levels.* J Biol Chem, 2010. **285**(16): p. 12416-25.
23. Lindstrom, M.S., *Emerging functions of ribosomal proteins in gene-specific transcription and translation.* Biochem Biophys Res Commun, 2009. **379**(2): p. 167-70.
24. Greco, A., *Involvement of the nucleolus in replication of human viruses.* Rev Med Virol, 2009. **19**(4): p. 201-14.
25. Latonen, L., et al., *Proteasome inhibitors induce nucleolar aggregation of proteasome target proteins and polyadenylated RNA by altering ubiquitin availability.* Oncogene, 2010. **30**(7): p. 790-805.
26. Latonen, L., *Nucleolar aggresomes as counterparts of cytoplasmic aggresomes in proteotoxic stress.* Bioessays, 2011. **33**(5): p. 386-395.
27. Abella, N., et al., *Nucleolar disruption ensures nuclear accumulation of p21 upon DNA damage.* Traffic, 2010. **11**(6): p. 743-55.
28. Hutten, S., et al., *An intranucleolar body associated with rDNA.* Chromosoma, 2011. **120**(5): p. 481-99.
29. Porter, D.C., et al., *Cyclin-dependent kinase 8 mediates chemotherapy-induced tumor-promoting paracrine activities.* Proc Natl Acad Sci U S A, 2012. **109**(34): p. 13799-804.
30. Weinberg, R.A., *The retinoblastoma protein and cell cycle control.* Cell, 1995. **81**(3): p. 323-30.
31. Sherr, C.J. and J.M. Roberts, *Inhibitors of mammalian G1 cyclin-dependent kinases.* Genes Dev, 1995. **9**(10): p. 1149-63.

32. Serrano, M., G.J. Hannon, and D. Beach, *A new regulatory motif in cell-cycle control causing specific inhibition of cyclin D/CDK4.* Nature, 1993. **366**(6456): p. 704-7.
33. Kaelin, W.G., Jr., *Functions of the retinoblastoma protein.* Bioessays, 1999. **21**(11): p. 950-8.
34. Ruas, M. and G. Peters, *The p16INK4a/CDKN2A tumor suppressor and its relatives.* Biochim Biophys Acta, 1998. **1378**(2): p. F115-77.
35. Alcorta, D.A., et al., *Involvement of the cyclin-dependent kinase inhibitor p16 (INK4a) in replicative senescence of normal human fibroblasts.* Proc Natl Acad Sci U S A, 1996. **93**(24): p. 13742-7.
36. Stein, G.H., et al., *Differential roles for cyclin-dependent kinase inhibitors p21 and p16 in the mechanisms of senescence and differentiation in human fibroblasts.* Mol Cell Biol, 1999. **19**(3): p. 2109-17.
37. Jacobs, J.J., et al., *The oncogene and Polycomb-group gene bmi-1 regulates cell proliferation and senescence through the ink4a locus.* Nature, 1999. **397**(6715): p. 164-8.
38. Cantley, L.C. and B.G. Neel, *New insights into tumor suppression: PTEN suppresses tumor formation by restraining the phosphoinositide 3-kinase/AKT pathway.* Proc Natl Acad Sci U S A, 1999. **96**(8): p. 4240-5.
39. Jimenez, C., et al., *Identification and characterization of a new oncogene derived from the regulatory subunit of phosphoinositide 3-kinase.* EMBO J, 1998. **17**(3): p. 743-53.
40. Li, D.M. and H. Sun, *PTEN/MMAC1/TEP1 suppresses the tumorigenicity and induces G1 cell cycle arrest in human glioblastoma cells.* Proc Natl Acad Sci U S A, 1998. **95**(26): p. 15406-11.
41. Tresini, M., et al., *A phosphatidylinositol 3-kinase inhibitor induces a senescent-like growth arrest in human diploid fibroblasts.* Cancer Res, 1998. **58**(1): p. 1-4.
42. Zhang, Y., Y. Xiong, and W.G. Yarbrough, *ARF promotes MDM2 degradation and stabilizes p53: ARF-INK4a locus deletion impairs both the Rb and p53 tumor suppression pathways.* Cell, 1998. **92**(6): p. 725-34.
43. Ferbeyre, G., et al., *PML is induced by oncogenic ras and promotes premature senescence.* Genes Dev, 2000. **14**(16): p. 2015-27.
44. Pearson, M., et al., *PML regulates p53 acetylation and premature senescence induced by oncogenic Ras.* Nature, 2000. **406**(6792): p. 207-10.
45. Dotto, G.P., *p21(WAF1/Cip1): more than a break to the cell cycle?* Biochim Biophys Acta, 2000. **1471**(1): p. M43-56.
46. Gartel, A.L. and A.L. Tyner, *The growth-regulatory role of p21 (WAF1/CIP1).* Prog Mol Subcell Biol, 1998. **20**: p. 43-71.
47. Niculescu, A.B., 3rd, et al., *Effects of p21(Cip1/Waf1) at both the G1/S and the G2/M cell cycle transitions: pRb is a critical determinant in blocking DNA replication and in preventing endoreduplication.* Mol Cell Biol, 1998. **18**(1): p. 629-43.
48. Chang, B.D., et al., *p21Waf1/Cip1/Sdi1-induced growth arrest is associated with depletion of mitosis-control proteins and leads to*

abnormal mitosis and endoreduplication in recovering cells. Oncogene, 2000. **19**(17): p. 2165-70.
49. Perkins, N.D., et al., *Regulation of NF-kappaB by cyclin-dependent kinases associated with the p300 coactivator.* Science, 1997. **275**(5299): p. 523-7.
50. Asada, M., et al., *Apoptosis inhibitory activity of cytoplasmic p21(Cip1/WAF1) in monocytic differentiation.* EMBO J, 1999. **18**(5): p. 1223-34.
51. Chang, B.D., et al., *Role of p53 and p21waf1/cip1 in senescence-like terminal proliferation arrest induced in human tumor cells by chemotherapeutic drugs.* Oncogene, 1999. **18**(34): p. 4808-18.
52. Chang, B.D. and I.B. Roninson, *Inducible retroviral vectors regulated by lac repressor in mammalian cells.* Gene, 1996. **183**(1-2): p. 137-42.
53. Chang, B.D., et al., *Effects of p21Waf1/Cip1/Sdi1 on cellular gene expression: implications for carcinogenesis, senescence, and age-related diseases.* Proc Natl Acad Sci U S A, 2000. **97**(8): p. 4291-6.
54. Hayflick, L. and P.S. Moorhead, *The serial cultivation of human diploid cell strains.* Exp Cell Res, 1961. **25**: p. 585-621.
55. Mathon, N.F. and A.C. Lloyd, *Cell senescence and cancer.* Nat Rev Cancer, 2001. **1**(3): p. 203-13.
56. Vaziri, H., et al., *ATM-dependent telomere loss in aging human diploid fibroblasts and DNA damage lead to the post-translational activation of p53 protein involving poly(ADP-ribose) polymerase.* EMBO J, 1997. **16**(19): p. 6018-33.
57. von Zglinicki, T., *Telomeres and replicative senescence: Is it only length that counts?* Cancer Lett, 2001. **168**(2): p. 111-6.
58. Di Leonardo, A., et al., *DNA damage triggers a prolonged p53-dependent G1 arrest and long-term induction of Cip1 in normal human fibroblasts.* Genes Dev, 1994. **8**(21): p. 2540-51.
59. Serrano, M., et al., *Oncogenic ras provokes premature cell senescence associated with accumulation of p53 and p16INK4a.* Cell, 1997. **88**(5): p. 593-602.
60. Zhu, J., et al., *Senescence of human fibroblasts induced by oncogenic Raf.* Genes Dev, 1998. **12**(19): p. 2997-3007.
61. Campisi, J., *Cellular senescence as a tumor-suppressor mechanism.* Trends Cell Biol, 2001. **11**(11): p. S27-31.
62. Dimri, G.P., et al., *A biomarker that identifies senescent human cells in culture and in aging skin in vivo.* Proc Natl Acad Sci U S A, 1995. **92**(20): p. 9363-7.
63. Kurz, D.J., et al., *Senescence-associated (beta)-galactosidase reflects an increase in lysosomal mass during replicative ageing of human endothelial cells.* J Cell Sci, 2000. **113 (Pt 20)**: p. 3613-22.
64. Vogt, M., et al., *Independent induction of senescence by p16INK4a and p21CIP1 in spontaneously immortalized human fibroblasts.* Cell Growth Differ, 1998. **9**(2): p. 139-46.

65. McConnell, B.B., et al., *Inhibitors of cyclin-dependent kinases induce features of replicative senescence in early passage human diploid fibroblasts.* Curr Biol, 1998. **8**(6): p. 351-4.
66. Gilbert, L.A. and M.T. Hemann, *DNA damage-mediated induction of a chemoresistant niche.* Cell, 2010. **143**(3): p. 355-66.
67. Yamauchi, K., et al., *Induction of cancer metastasis by cyclophosphamide pretreatment of host mice: an opposite effect of chemotherapy.* Cancer Res, 2008. **68**(2): p. 516-20.
68. Shaked, Y., et al., *Therapy-induced acute recruitment of circulating endothelial progenitor cells to tumors.* Science, 2006. **313**(5794): p. 1785-7.
69. Shaked, Y., et al., *Rapid chemotherapy-induced acute endothelial progenitor cell mobilization: implications for antiangiogenic drugs as chemosensitizing agents.* Cancer Cell, 2008. **14**(3): p. 263-73.
70. Barcellos-Hoff, M.H. and S.A. Ravani, *Irradiated mammary gland stroma promotes the expression of tumorigenic potential by unirradiated epithelial cells.* Cancer Res, 2000. **60**(5): p. 1254-60.
71. Adler, A.S., et al., *CDK8 maintains tumor dedifferentiation and embryonic stem cell pluripotency.* Cancer Res, 2012. **72**(8): p. 2129-39.
72. Xu, W. and J.Y. Ji, *Dysregulation of CDK8 and Cyclin C in tumorigenesis.* J Genet Genomics, 2011. **38**(10): p. 439-52.
73. Fabian, M.A., et al., *A small molecule-kinase interaction map for clinical kinase inhibitors.* Nat Biotechnol, 2005. **23**(3): p. 329-36.
74. Firestein, R., et al., *CDK8 is a colorectal cancer oncogene that regulates beta-catenin activity.* Nature, 2008. **455**(7212): p. 547-51.
75. Morris, E.J., et al., *E2F1 represses beta-catenin transcription and is antagonized by both pRB and CDK8.* Nature, 2008. **455**(7212): p. 552-6.
76. Donner, A.J., et al., *CDK8 is a positive regulator of transcriptional elongation within the serum response network.* Nat Struct Mol Biol, 2010. **17**(2): p. 194-201.
77. Tewey, K.M., et al., *Adriamycin-induced DNA damage mediated by mammalian DNA topoisomerase II.* Science, 1984. **226**(4673): p. 466-8.
78. Chen, Q. and B.N. Ames, *Senescence-like growth arrest induced by hydrogen peroxide in human diploid fibroblast F65 cells.* Proceedings of the National Academy of Sciences, 1994. **91**(10): p. 4130-4134.
79. Goessens, G., M. Thiry, and A. Lepoint, *Relations between nucleoli and nucleolus-organizing regions during the cell cycle*, in *Chromosomes today*. 1987, Springer. p. 261-271.
80. Bringold, F. and M. Serrano, *Tumor suppressors and oncogenes in cellular senescence.* Exp Gerontol, 2000. **35**(3): p. 317-29.
81. Roninson, I.B., *Tumor cell senescence in cancer treatment.* Cancer Res, 2003. **63**(11): p. 2705-15.
82. Friedl, P., et al., *Migration of coordinated cell clusters in mesenchymal and epithelial cancer explants in vitro.* Cancer Res, 1995. **55**(20): p. 4557-60.
83. Bunz, F., et al., *Requirement for p53 and p21 to sustain G2 arrest after DNA damage.* Science, 1998. **282**(5393): p. 1497-501.

84. Haaf, T. and D.C. Ward, *Inhibition of RNA polymerase II transcription causes chromatin decondensation, loss of nucleolar structure, and dispersion of chromosomal domains.* Exp Cell Res, 1996. **224**(1): p. 163-73.
85. Adler, A.S., et al., *CDK8 maintains tumor dedifferentiation and embryonic stem cell pluripotency.* Cancer research, 2012. **72**(8): p. 2129-2139.
86. Myers, L.C. and R.D. Kornberg, *Mediator of transcriptional regulation.* Annu Rev Biochem, 2000. **69**: p. 729-49.
87. Akoulitchev, S., S. Chuikov, and D. Reinberg, *TFIIH is negatively regulated by cdk8-containing mediator complexes.* Nature, 2000. **407**(6800): p. 102-6.
88. Elmlund, H., et al., *The cyclin-dependent kinase 8 module sterically blocks Mediator interactions with RNA polymerase II.* Proc Natl Acad Sci U S A, 2006. **103**(43): p. 15788-93.